Unified value-based feedback, optimization and risk management in complex electric energy systems

Unified value-based feedback, optimization and risk resource management in complex electric energy systems

Cite this article as: Marija Ilic and Rupamathi Jaddivada, Unified value-based feedback, optimization and risk resource management in complex electric energy systems, Optimization and Engineering https://doi.org/10.1007/s11081-020-09486-y

Noname manuscript No.
(will be inserted by the editor)

Unified Value-based Feedback, Optimization and Risk Resource Management in Complex Electric Energy Systems

Marija Ilic · Rupamathi Jaddivada

Received: date / Accepted: date

Abstract The ideas in this paper are motivated by an increased need for systematic data-enabled resource management of large-scale electric energy systems. The basic control objective is to manage uncertain disturbances, power imbalances in particular, by optimizing available power resources. To that end, we start with a centralized optimal control problem formulation of system-level performance objective subject to complex interconnection constraints and constraints representing highly heterogeneous internal dynamics of system components. To manage spatial complexity, an inherent multi-layered structure is utilized by expressing interconnection constraints in terms of unified power variables and their dynamics. Similarly, the internal dynamics of components and sub-systems (modules), including their primary automated feedback control, is modeled so that their input-output characterization is also expressed in terms of power variables. This representation is shown to be key to managing the multi-spatial complexity of the problem. In this unifying energy/power state space, the system constraints are all fundamentally convex, resulting in the convex dynamic optimization problem, for typically utilized quadratic cost functions. Based on this, an interactive multi-layered modeling and control method is introduced. While the approach is fundamentally based on the primal-dual decomposition of the centralized problem, it is proposed for the first time to utilize sensitivity functions of distributed agents for solving the primal distributed problem. Iterative communication complexity typically required for convergence of point-wise information exchange is replaced by

M. Ilic
Laboratory of Information and Decision Systems, Massachusetts Institute of Technology
77 Massachusetts Avenue, Cambridge MA- 02139
E-mail: ilic@mit.edu

R. Jaddivada
Laboratory of Information and Decision Systems, Massachusetts Institute of Technology
77 Massachusetts Avenue, Cambridge MA- 02139
E-mail: rjaddiva@mit.edu

the embedded distributed optimization by the modules when creating these functions. A theoretical proof of the convergence claim is given. Notably, the inherent multi-temporal complexity is managed by performing model predictive control (MPC)-based decision making when solving distributed primal problems. The formulation enables distributed decision-makers to value uncertainties and related risks according to their preferences. Ultimately, the distributed decision making results in creating a bid function to be used at the coordinating market-clearing level. The optimization approach in this paper provides a theoretical foundation for next-generation Supervisory Control and Data Acquisition (SCADA) in support of a Dynamic Monitoring and Decision Systems (DyMonDS) framework for a multi-layered interactive market implementation in which the grid users follow their sub-objectives and the higher layers coordinate interconnected sub-systems and the high-level system objectives. This makes it conclusive when designing IT-enabled protocols for secure operations, planning, and markets.

Keywords Modeling · Complex electric energy systems · Control systems · Optimization · Reliable electric energy · Efficient electric energy systems · Electricity Markets

1 Introduction

This paper introduces a novel modeling and optimization approach for complex electric energy systems. The complexity is multi-fold. New technologies are being embedded within the legacy of electric energy systems. Also, subsystems have often conflicting sub-objectives which are a combination of technical, economic, business and cyber-security functions. One of the main challenges is how to capture the inter-dependencies within these rapidly changing systems. In this paper, we show that it is sufficient to characterize all components and sub-systems as triplets of power, rate of power and rate of reactive power needed by and/or provided to the rest of the system. This helps conceptualize the decision-making regarding interactions: (a) between components within any given subsystem, and (b) between subsystems within the interconnected system.

We show that protocols for interactive information exchange between complex technology-specific subsystems, on one hand, and the higher-layer aggregated entities, on the other, can be supported using only this triplet of variables referred to as the interaction variables. The subsystem-level automated control design in support of decisions to participate in power balancing and delivery at the rate determined by their specific technologies and preferences is posed as the problem of a multi-layered complex system design needed to meet interaction specifications. Today's balancing authorities (BAs) are an aggregate case of this more general architecture comprising all grid users (small prosumers, large conventional generators, renewable resources) as well as delivery systems (electrical microgrids, distribution, transmission, regional and multi-regional grids as well as gas, heat, and water). For this multi-layered

interactive approach to work, each grid user must belong to an intelligent Balancing Authority (iBA) unless it is completely disconnected.

It is suggested to further consider this modeling framework as the basis for next-generation SCADA which provides transparent information. Perhaps the compelling reason for moving forward with establishing protocols for supporting future operations, planning and markets using the proposed modeling approach is that these are effectively an outgrowth of specifications/standards used for automatic generation control (AGC) in today's industry. It is shown that the technically challenging extension of ACE to support balancing power at specific rates over time-horizons relevant for stable operation without experiencing fast sub-transient (mechanical, electro-magnetic) resonance or transient instability is closely related to the problem of controlling rate of change of instantaneous real power imbalances. These are further used to stress the fundamental relevance of fast power electronic switching, fast storage, and non-linear control so that specifications of fast interactions by the iBAs can be implemented. Much the same way as with the ingenious Automatic Generation Control(AGC), it becomes possible to operate the system by specifying performance in terms of ACE-like variables, now for all iBAs and over a stratum of temporal horizons [1].

Today's reliability and cyber-security standards can and should evolve into more flexible protocols supported by this framework. It is even possible to compute boundaries of the iBAs dynamically, which would make it practically impossible for the intruders to corrupt the critically-needed information. Therefore, it becomes possible to manage complexity by protecting only the information important for operations in a cyber-secure manner.

1.1 Contributions

We propose new formulations that help manage these complex energy systems without any a priori simplifications, as prevalent in today's methods. The contributions of this paper are multi-fold:

First, the application of a general modeling framework proposed in [2] is utilized to model interactions of electric energy systems. This modeling is unified and is based on the general conservation laws, thus overcoming the complexity of modeling for power system operations, markets and analysis, irrespective of its size and the heterogeneity of the components and/or their aggregates.

Second, new formulations have been proposed to ensure that the decision-making framework is in alignment with the underlying physics. These formulations are further shown to be convex with linear constraints when the component specifications are all in terms of the interaction variables. As a result, optimal control with unique global optimum can be found, if there exists at least one feasible operating point. The interactive nature of modeling, coupled with the protocols proposed serves as the basis for implementability of the commitments made by each of the decision-making hierarchical layers.

Third, we provide a theoretical foundation for DyMonDS supporting novel decomposition strategy wherein the agents and/or groups of agents exchange minimal information with their aggregators/coordinators. This minimal information is in the form of sensitivity functions for prices, instead of the points used in state-of-the-art decomposition strategies. Due to the minimal coordination and the quadratic assumption of the bid curves, we show that convergence of system-level objective functions at a rate of $\mathcal{O}(1/k)$ can be achieved.

Finally, it is proposed to utilize the modeling framework supplemented with DyMonDS-based decomposition strategy to assess the trade-offs with regards to risks taken by the agents through embedded model predictive control versus the coordinator assuming the risk through multi-temporal markets involving information exchange through the triplets of power, rate of power and rate of reactive power.

Most importantly, one should note that our proposed methods can be embedded within existing SCADA in power grids without much-added hardware deployment. According to the best of authors' knowledge, the interactive approach to efficiently operating electric energy systems through implementable protocols is first of its kind.

1.2 Outline

The paper is organized as follows: We begin with a brief overview of the existing literature on the study of complex energy systems in Section 2. We next pose the problem and describe the need to establish consistent and transparent protocols, for operating such complex systems. It is, in particular, a difficult task to align the sub-objectives of technologically and socially diverse decision-makers with the grid-level objectives [3]. The hurdles involved in managing these systems are presented on a hypothetical grid as an example in Section 3. We propose to utilize the modeling framework proposed in [2] in the context of these complex energy systems to facilitate the integration of heterogeneous devices efficiently. It is important to note that the changing energy systems are always subject to ever-changing disturbances entering the grid, and thus it becomes important to characterize the dynamic inefficiency as the agents interact with one another. The modeling framework along with the characterization of dynamic inefficiencies and interconnected system stability conditions proposed in [2, 4] have been reviewed in Section 4. We further elaborate on certain elements of the modeling framework that assist the generalization of today's AGC. Here we also highlight how the modeling of instantaneous reactive power dynamics at the interfaces can help characterize both inefficiencies and the passivity conditions.

We next pose the problem for managing heterogeneous agents within each iBA and/or to coordinate multiple iBAs, as a continuous-time optimal control problem subject to dynamic constraints in energy space in Section 5. The linearity of the coupling constraints in energy space is utilized to propose a novel decomposition technique through minimal coordination. This algorithm

and the associated sub-problems to be solved by the agents and the coordinators are formulated in Section 6. It is shown that the optimization problems for coordinating interactions within or across iBAs become linear convex optimization problems in the energy space. This is true as long as specifications of iBAs are in terms of interaction variables. The resulting system equilibrium is shown to be near-optimal in an average sense over coordination time intervals. The convergence analysis of such spatial decomposition method is provided in Appendix A.

In Section 7, we elaborate upon how multi-temporal disturbance predictions can be accounted for in the continuous-time problem posed. The risks associated with future availability of the energy resources can either be completely assumed by coordinators, maintaining enough reserves for *just-in-case* type of uncertainty. Alternatively, the problem can be formulated as a *wait-and-see* type of uncertainty, facilitating agents themselves to submit bids to make profits for the future possible shortage of energy resources, based on their risk margins. Often the former is a better option for smaller grids such as microgrids, while the latter can be considered similar to the approach taken by today's bidding strategies of large generators. The interactive framework facilitates such trade-off analysis in a transparent manner through the proposed protocols. The results are heavily dependent on the availability of the disturbance predictions and its variation, characteristics of the agents, and how risk-averse the entities are. Such a discussion in the context of these energy systems is offered in Section 7. Notably, this interactive modeling and control framework lends itself to monetization of the risks taken by the different agents and/or their iBAs.

Only a few examples of the usage of the proposed modeling framework that could exploit the inherent complexity of the grids to its advantage are provided. The scope and applicability of such an approach are enormous and can be utilized towards various other aspects of energy systems including efficient investment planning, cybersecurity, state estimation, computer architecture design and many more. Some of these future research directions are discussed in Section 8. In Section 9, a few recommendations are made for further discussion of the proposed energy-space based next generation SCADA and protocols for enabling reliable and efficient data-enabled electricity services at a value. It is pointed out that this general proposal was made to FERC in an invited testimony on the state of reliability, and that the recommendation was made to work closer with industry to pursue it for further adoption [5]. It is with this in mind that this paper is written to motivate further consideration of the proposed framework.

2 Related work

Future electric energy systems will comprise multi-physics energy conversion equipment, resources and loads, interfaced with the electric energy delivery system. Presently these systems are not modeled as end-to-end systems. Most

literature on energy systems can be broadly categorized into two paths of research: component-level and system-level. Each of the components ranging from the large-scale generators to that of demand-side water heater devices has been studied extensively for their ability to control output specifications, such as the nominal frequency and voltage in generators and permissible temperatures in electrical water heaters [6–11]. These components, however, have not been designed to satisfy the specifications on interactions with the grid, which are of importance for system-level studies [3]. Given the sheer size of these systems, the study of the interactions of component-specific dynamics with that of the interactions in the system has always been represented as a major challenge [11, 12].

2.1 Modeling and control

From the systems perspective, traditionally power grids have been studied by utilizing Thevenin and Norton's equivalent circuits recomputed every timestep, the accuracy of which depends on the chosen interaction protocols and are generally not scalable to very large systems. [1] has proposed a scalable two-tier flocking-based protocol for ensuring transient stability of large power grids. This study, however, begins with a Kron-reduced network for assessing the generator-induced instabilities alone. This has been a valid approach in the past when the disturbances entering the grid such as those from the renewables and did not form a high fraction of the generation portfolio.

Another complexity arises as the future evolution of the disturbances has to be taken into account. Such time-coupled constraints have been handled in the past for hydro-thermal scheduling in large scale power systems, which have been extended to batteries utilized in energy management as well [13]. Especially with the passing of the FERC order 841 for the inclusion of storage in market operations, rapid development and deployment of storage are becoming a reality [14]. While the system-level problem is more complex due to time-coupled dynamic constraints of the batteries, a large number of papers proposing variants of dynamic programming are being written for solving such problems efficiently [15–19].

The need to consider more granular modeling for system-level studies has been realized with the advent of IoT devices, particularly in retail markets and distribution grid operations [20, 21]. This increases the problem complexity because of a large number of decision variables and constraints. Most system-level studies have targeted a specific temporal and spatial scale to either perform market design and/or design control strategies. For instance, the protocols for control design to ensure stable operation of smaller electric power grids, capable of operating autonomously, also referred to as microgrids, have been studied in [22–29]. The distribution grids coordinating millions of small KW-level devices have been studied in the context of quantifying the aggregate flexibility [30–34].

2.2 Resolving computational complexity

Typically the benchmark problems for the energy management are non-convex. To apply any decomposition strategy, these constraints are all simplified by applying convex approximations [35–38]. There exist a few papers on the decoupled real and reactive power flow analysis as well [39, 40]. A few other approaches include use of auxiliary gradient system, holomorphic embedding and homotopy-based methods [41–44]. These approaches, however, are not scalable. Furthermore, recent literature on distribution grids utilizes simplified network models, valid only for the radial networks [45–49]. A few studies have focused on solution approaches to decrease the solution time and minimize the duality gap [50–52]. Most literature on the coordination of small end-users that suffer the curse of dimensionality has focused on the usage of real power flow constraints alone[53].

Realizing the inherent spatial complexity, several decomposition methods have traditionally been utilized in power grids [54]. Augmented Lagrangian relaxation schemes have been introduced to ensure convexity of the decomposed problems, resulting in a class of numerical methods called Alternating Direction Method of Multipliers (ADMM) [55]. Proximal methods which are a generalization of ADMM methods have gained a lot of attention in recent years. As a result. several advancements in ADMM have been proposed in the past two decades to decrease the solution time and number of iterations for convergence [56]. [45] has proposed a proximal message passing scheme to solve the optimal power flow problem with dynamic constraints of batteries through a peer-to-peer communication architecture. This work, however, fails to consider other types of heterogeneous DERs and also its decentralized algorithm utilizes point-by-point updates, requiring a larger number of iterations for convergence. Several other decentralized and distributed schemes for energy management have been proposed [57–63]. While some of these papers extend the architecture to a hierarchical setting, they do not consider the effect of internal control design and its saturation on the system-level performance.

2.3 Accounting for uncertainties and risks

While most of the research is targeted towards the deterministic setting, the net inflexible demand, in general, can not be predicted accurately enough. As a result, several stochastic and robust optimization strategies have also been developed for large scale power systems to manage utility-scale uncertainties in wind, solar and demand forecasts. [64–68]. In the distribution grids, stochastic formulations have been proposed through bin-based models for characterizing the approximate aggregate performance of homogeneous distributed energy resources (DERs) [69–71]. The performance of this is however contingent upon the law of large numbers [30, 31]. A few other studies in the literature have relied on utilizing fast expensive batteries to ensure aggregate performance by also considering uncertainties in retail market prices[32, 72, 73]. A compara-

tive analysis of demand response utilizing stochastic and robust optimization methods have been done in [74] by considering price uncertainty. A few other have taken an approach to characterize flexibility of an aggregation of small end-users by characterizing the upper and lower bounds of the aggregate consumption variation ahead of time [75]. But all of these studies considered prosumers as price-takers without accounting for local device level uncertainties and their willingness to offer grid services.

2.4 Implementation of markets

Existing literature overlays market design on top of these complex systems through non-transparent protocols of the grid entities. Present-day operations procure reserves at different timescales to be able to cater to unpredictable disturbances. Today this is being done by activating several additional generators without actually supplying any load and are referred to as Reliability Must-Run (RMR) units [76]. Procuring these resources thus incurs additional costs referred to as uplift or out-of-merit scheduling costs, which get reflected in the form of increased electricity bills. The procurement of resources is also done irrespective of the internal control design schemes. As a result, the component commitments are only often estimated but not implementable, resulting in inefficient operations [76, 77]. In particular, the commitments made by the entities are not aligned with the control objectives of these components. This makes the adherence to market commitments questionable, in light of the non-stationary disturbances entering the components both from the grid and from the external environment at different timescales.

A variety of pricing rules have been studied to support efficient market operations. Multi-period markets have been studied in [78, 79]. The non-convexities associated with start-up, shut-down, and several other non-convexities result in mixed-integer linear programming problem that can not be mapped to appropriate pricing schemes and so there have been several studies on relaxation techniques for each of these convexities to then deduce a transparent pricing mechanism. These methods are mostly not scalable [80, 81]. At present, there exist only standards for operating large scale electric power grids; there are no well-defined protocols for supporting interactions between the DERs embedded within the balancing authorities. As the number and type of small DERs embedded into distribution and microgrids increases, it is important to have information exchange between different layers within complex balancing authorities at different spatio-temporal levels.

2.5 Dynamic problems

Furthermore, most of the existing studies assume perfect stabilizing control at the component level for all operating conditions. System-level stability studies are performed only minimally in light of the static decisions made, and further such assessment is only performed by applying various network reduction

techniques, thus leaving the grid vulnerable to unforeseen operating conditions [3]. In order to emulate these interactions, there has been increased interest in simulating the detailed component dynamics while modeling dynamics of external environment [82–85]. More and more hardware-in-loop tests beds are being conducted to analyze the effect of fast power electronic controllers on smaller microgrids [86–88]. There however are lack of systematic methods to ensure stable operation of even these smaller sized general topology of the microgrids [25, 61]. What is needed is a simple yet unified approach to managing these complex energy systems by suitably defining protocols for operations, control and risk mitigation in response to multi-rate and multi-spatial disturbances seen.

In this paper, we recognize the fundamental difficulties underlying the complexity of these complex systems. In particular, there is no alignment between the data exchanged and the existing software used for energy management, on one hand, and the performance objectives, such as efficiency, reliability, cyber-security, and resiliency, on the other. Fundamentally, the question arises concerning minimal specifications needed for information exchange so that when coordination is carried out using this information the interconnected system "works".

3 Problem posing and the challenges involved

Shown in Fig. 1 is a conceptual representation of two BAs (shown in red boxes) responsible for compensating energy imbalances seen by each area. These energy imbalances are known as the Area Control Error (ACE), caused by a combination of each BA load deviations from the forecast and by the deviations of energy exchanges from the pre-agreed on schedules by the BAs. The BA-level feedback function known as the Automatic Generation Control (AGC) is responsible for ensuring that ACE crosses zero once 10 minutes. This standard is expected to ensure that QoS measured in terms of frequency deviations from its nominal value if ACE crosses zero on a 10-minute basis. The assumption made is that ACE is generally a zero-mean deviation during this period. At a much faster time scale, it is assumed that generators being the only truly controlled components have local automation to control frequency and voltage to their setpoints. This, again, assumes that disturbances around operating conditions for which the PID automation was tuned are small. Frequency dynamics is governed by the mismatch of mechanical power applied to the rotor shaft of a generator and of electrical power consumed at its terminals. The rate at which frequency oscillates depends on the inertia of the power plant, according to Newton's law. The governor changes this rate of response in closed-loop in response to frequency deviation from the governor control set point. The approach utilized today is not necessarily implementable.

Furthermore, at a finer granularity, each of the areas in the red boxes may represent small microgrids with heterogeneous components interconnected through smaller microgrids. Some form of energy conversion (mechanical to electrical;

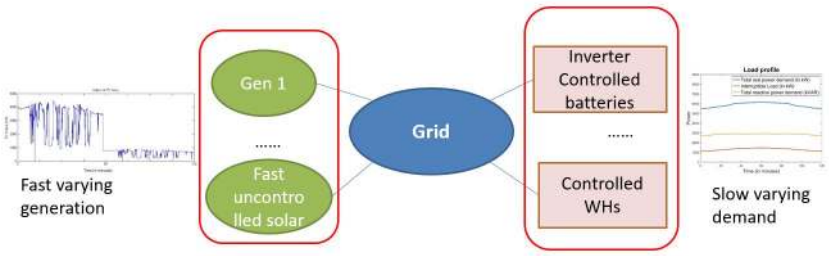

Fig. 1 Generation and demand changing at varying rates in the two areas

chemical to electrical) takes place internally within a component, and the internal energy converted to the electrical energy gets sent and delivered via the electric power grid. With the changing energy systems, modeling new technologies are becoming quintessential, since they may have a significant effect on the reliability and efficiency of an end-to-end electric energy system. However, representing sufficiently detailed models of such a heterogeneous system is practically impossible. In particular, different resources are manufacturer-specific and often the details of internal technology are not made known to the users. This fundamental dichotomy is the main reason for the unified multi-layered modeling approach, that we propose to utilize the general modeling framework in [2] to model the interactions of multi-physics components and their aggregates.

Typically, some of these components within the red boxes in Fig. 1 are controllable while the rest are uncontrollable and are seen as disturbances that can be predicted at multiple spatial and temporal scales with varying levels of accuracy. Furthermore, the controllable components can not instantaneously ramp-up and down their real power injections, resulting in supply-demand imbalance creating frequency and voltage excursions that affect the Quality of Response (QoR). Most of the hierarchical control attempts to balance real power supply and demand, and it assumes that the reactive power is such that the power delivery is feasible and stable within the frequency and voltage limits allowed by the equipment manufacturers. Therefore, it is assumed that reactive power deviations do not affect significantly real power dynamics, therefore control of frequency and voltage utilize decoupled models. These models and resultantly traditionally utilized decision-making software with embedded unit commitment or AC optimal power flow are all static in nature. They can not be utilized to ensure that the rates of changes in power injections exactly match. For instance, consider the net generation and consumption seen in the higher layers in Fig. 1 where a fast solar power plant is injecting power into a rather slow varying demand. This interconnection is not feasible and may lead to unstable operation. We show with the proposed modeling framework how the consideration of interaction dynamics can significantly affect the maximum power transferable through a wire later in this section. We thereby also define

the notion of dynamic inefficiencies that restrict the real power transfer that produces useful work.

Also, the modeling language used in the large scale electric power grids has been the one in which amplitudes and phase angle deviations of the sinusoidal currents and voltages are much slower than their nominal frequency carrier. This fundamentally allows for an algebraic relation between effort and flow amplitudes and phases, and, furthermore, to use of complex-valued relations between these variables. This modeling assumption, while somewhat hidden and overlooked, is one of the key roadblocks to designing provably stable fast switching nonlinear control. As a result, there have been recent occurrences of sub-synchronous electromagnetic resonance between power electronically switched control in wind power plants and the near-by series capacitors control of transmission line inductances [89].

In addition, the markets are overlaid on top of these grids wherein there may exist a wholesale market to coordinate the transactions at the higher granularity and retail markets to clear the transactions within each micro-grid. Today standard protocols only exist for wholesale markets, wherein the coordinator assumes the risk of ensuring a sufficient number of resources are available. This may be done over varying timescales and the incentives and price signals for these resources are all quite arbitrary. The complexity in models and the non-convexity leading to a different primal-dual solution is a prime cause for not having economic signals aligned with the technical ones.

At the conceptual level, in our modeling approach, any complex multi-temporal multi-spatial heterogeneous electric energy system is represented by modeling layers as the entities responsible for their performance in as much detail as decided on by these entities. In what follows we introduce this multi-layer modeling. We show how complex models of equipment and groups of interconnected equipment can be derived by starting from detailed internal dynamics and mapping it into dynamics relevant for deriving dynamic interactive models of interconnected modules expressed in terms of common variables we call interaction variables. This principle of modeling enables unified modeling of interconnected systems without excessive complexity. It is shown in this paper how this modeling can be used to support systematic optimization and control at distributed layers, and, how can the interactive model be used to enable the integration of otherwise physically heterogeneous modules with qualitatively different sub-objectives.

4 Review of the modeling framework

The dynamic model of each component can be expressed in a standard state-space form [90].

$$\begin{aligned} \dot{x}_i &= f'_{x,i}\left(x_i, u_i, m_i, r_i\right) \qquad x_i(0) = x_{i,0} \\ y_i &= f'_{y,i}\left(x_i, u_i, m_i, r_i\right) \end{aligned} \tag{1}$$

where $x_i(t) \in \mathcal{X}_i$, $u_i(t) \in \mathcal{U}_i$, $m_i(t) \in \mathcal{M}_i$ and $r_i(t) \in \mathcal{R}_i$ denote local states, inputs, local disturbances and port inputs belonging to respective manifolds denoted as $\mathcal{X}_i, \mathcal{U}_i, \mathcal{M}_i, \mathcal{R}_i$. Variable $y_i(t)$ denotes local outputs of interest, typically frequency and voltage as the key indicators of QoS. A subset of the state variables appear at the ports of the components which may be either flow-type $f_i \in \mathcal{F}_i$ or effort-type $e_i \in \mathcal{E}_i$ variables. These variables are further associated with respective conjugate variables which would be a flow-type $e_i \in \mathcal{F}_i^*$ or effort-type variable $f_i \in \mathcal{E}_i^*$ respectively [91, 92]. At the ports, one of these pairs is local to the component, while the other is dictated by its interconnection to the rest of the system, also defined as the port inputs in Eqn. (1). More precisely, if the effort variable is a port state i.e. $e_i \in \mathcal{X}_i$, this implies, its pair $f_i \in \mathcal{R}_i$.

The quantities of instantaneous real and reactive power appearing at any of the ports characterized by respective effort and flow variables as shown in Eqns. (2a) and (2b) [93]

Instantaneous real and reactive power:

$$P_i = e_i^T f_i \qquad \forall\, (e_i, f_i) \in \mathcal{E}_i \times \mathcal{F}_i \tag{2a}$$

$$\dot{Q}_i = {e_i}^T \tfrac{df_i}{dt} - {f_i}^T \tfrac{de_i}{dt} \qquad \forall \left((e_i, \dot{e}_i), \left(f_i, \dot{f}_i\right)\right) \in \mathcal{TE}_i \times \mathcal{TF}_i \tag{2b}$$

Here, $\mathcal{TE}_i \times \mathcal{TF}_i$ is the tangent manifold of the effort and flow variables at the port of component i respectively [2]. The state variables can be utilized to define the stored energy E_i, stored energy in tangent space $E_{t,i}$, real power in tangent space $P_{t,i}$, time constant τ_i, as follows: [2, 94]

$$\begin{aligned} E_i &= \tfrac{1}{2} {x_i}^T H_i x_i & E_{t,i} &= \tfrac{1}{2} \tfrac{dx_i}{dt}^T H_i \tfrac{dx_i}{dt} \\ \tau_i &= \tfrac{E_i(x_i)}{D_i(x_i)} & P_{t,i} &= \tfrac{de_i}{dt}^T \tfrac{df_i}{dt} \end{aligned} \tag{3}$$

Here $D_i(x_i)$ is the damping function indicating the dissipative losses [2]. More formal definitions of these quantities for non-linear systems can be referred to in [2], starting from the fundamental circuit element characterization [95]. With these definitions, it was shown in [2] that the pairs of effort and flow variables (e_i, f_i) can be directly mapped to the instantaneous real and reactive power through a diffeomorphic mapping. As a result, the model in Eqn. 1 can be re-written as:

Stand-alone model for control design:

$$\begin{aligned} \dot{x}_i(t) &= f_{x,i}\left(x_i(t), u_i(t), m_i(t), P_i(t), \dot{Q}_i(t)\right) \\ y_i(t) &= f_{y,i}\left(x_i(t), u_i(t), m_i(t), P_i(t), \dot{Q}_i(t)\right) \end{aligned} \tag{4}$$

Remark 1 *The term $P_{t,i}$ can also be approximated as the error made in approximating the time derivative of $\dot{P}_i$ through first-order discretization. If δt is the time interval used for discretization,*

$$P_{t,i}(t) = \frac{P_i(t) - P_i(t - \delta t)}{\delta t} - \dot{P}_i(t) \tag{5}$$

While this model is suitable for designing the control with specifications of the interactions P_i and $\dot{Q}_i$, it is too complex for understanding interactions across components. We thus define a simple enough interaction model for capturing interactions across components alone. With these definitions, the following interaction model is derived [2]:

Interaction model in energy space:

$$\dot{E}_i = P_i - \frac{E_i}{\tau_i} = p_i \tag{6a}$$

$$\dot{p}_i \;\; = 4E_{t,i} - \dot{Q}_i \tag{6b}$$

The dynamics of the interaction variable $z_i = [E_i,\ p_i]$, where $p_i = \dot{E}_i$ captures the dynamics of internal energy conversion independent of the type of energy conversion. The concept of interaction variables was first pursued in [39] and has appeared in several other works later on [3, 84, 96–98]. It is however for the first time in [2] that it has been possible to capture both real and reactive power dynamical interactions. While the variables E_i, p_i are referred to as the interaction variable dynamics of the sub-system, they are driven by the interactions from the neighbors quantified through real and reactive power inputs. Shown in Fig. 2 is the representation of a stand-alone component in the energy and power space. The bottom layer with the detailed

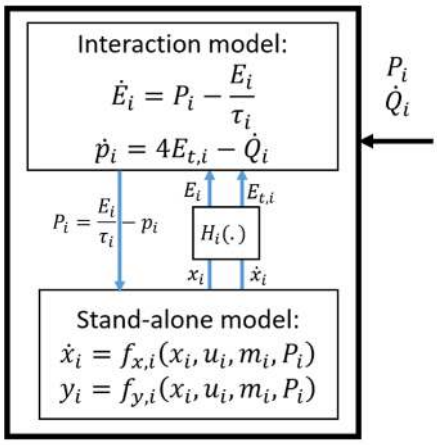

Fig. 2 Stand-alone component in open loop in energy space [2]

dynamics is utilized for designing control in energy and power space, while the input-output interactions alone are characterized by the higher-layer model. In the context of the conceptual diagram in Fig. 1, each of the components within the red boxes can be modeled as in Fig. 2.

Remark 2 *The model in Eqn.* (6) *can be extended to include dynamics of stored energy in tangent space as well, by utilizing the definition of* $P_{t,i}$*. For certain class of systems, this relation was derived in [94]. This is specially*

modeled when the information of internal dynamics is not available and can only be approximated through the time constants instead.

Extended Interaction model in energy space:

$$\dot{E}_i = -\frac{E_i}{\tau_i} + P_i = p_i \tag{7a}$$
$$\dot{p}_i \quad = 4E_{t,i} - \dot{Q}_i \tag{7b}$$
$$\dot{E}_{t,i} \quad = -\frac{E_{t,i}}{\tau_i} + P_{t,i} \tag{7c}$$

Clearly, this model requires information of $P_i, \dot{P}_i$ and $\dot{Q}_i$ from the neighbors to emulate the interaction dynamics, since $P_{t,i}$ can be recovered given the information of P_i and $\dot{P}_i$.

From the application of generalized Tellegen's theorem, all the three quantities obey the conservation law at memoryless intersections with neighbors [99]. Thus, if $\mathcal{C}_i$ denotes the set of neighboring components of i

$$P_i + \sum_{j\in\mathcal{C}_i} P_j = 0 \qquad \dot{P}_i + \sum_{j\in\mathcal{C}_i} \dot{P}_j = 0 \qquad \dot{Q}_i + \sum_{j\in\mathcal{C}_i} \dot{Q}_j = 0 \tag{8}$$

Furthermore, the component i further computes its own output variables $P_i^{out}, \dot{Q}_i^{out}$ for use by the neighbors, possibly with some time delay δt as

$$\begin{array}{l} P_i^{out}(t+\delta t) = \frac{dE_i(t)}{dt} + \frac{E_i(t)}{\tau_i} = p_i(t) \\ \frac{dQ_i^{out}}{dt}(t+\delta t) = \frac{dp_i(t)}{dt} - 4E_{t,i}(t) \\ \frac{dP_i^{out}}{dt}(t+\delta t) = \frac{P_i(t)-P_i(t-\delta t)}{\delta t} - \left(\frac{dE_{t,i}(t)}{dt} + \frac{E_{t,i}(t)}{\tau_i}\right) \end{array} \tag{9}$$

4.1 Aggregate models in energy space:

A multi-layered model comprises several sub-systems Σ_I which themselves could contain several interconnected components $i \in I$. An end-to-end system with such subsystems I can be modeled using the proposed energy space by characterizing each component in terms of its interaction variable z_I dynamics introduced in Eqn. 4 above. Each subsystem model shown in Fig. 3 is characterized in terms of the net instantaneous real power P_I and the rate of net instantaneous reactive power $\dot{Q}_I$. At the highest level the dynamics of interactions between subsystems within a complex system is expressed using the interaction variables between the sub-systems. The additivity of the interaction variables thus allows one to capture dynamics of interactions of aggregate entities, in a rather straight forward manner.

Recall the two-area electric power grid shown in Fig. 1. Today's industry approach to regulating frequency has been for each BA to cancel out their own ACE. Since each BA controls its ACE, the system comprising these two BAs are completely decoupled and competitive. Moreover, rates at which energy is stored and dissipated in each area and controlling ACE in a quasi-static way does not ensure that faster inter-area oscillations would not occur during the

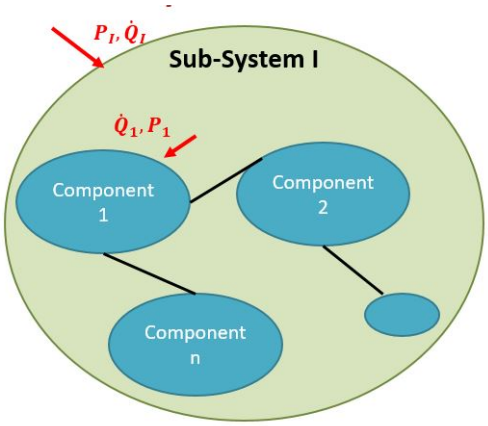

Fig. 3 A subsystem model in energy space

period $[kT_t]$, typically 10 minutes. It begins to become clear using energy space modeling that if the rates of change of reactive power in two control areas are vastly different, these inter-area oscillations will occur. They represent swings between the rate of power exchanged between the two areas.

4.2 Premise for the selection of interaction variables

It can be seen from the conceptual sketch of an electric power grid in Fig. 1, that future power grids will comprise of inverter controlled distributed energy resources (DERs), solar PVs and wind power plants, in particular. There has been extensive research done on modeling Newton's law-like dynamics of inverter controlled solar PVs or batteries. Instead of using physical inertia, a notion of "synthetic" inertia is introduced [100]. We observe that this inertia is generally used as a proxy to rates at which energy is generated or consumed. Modeling of such heterogeneous end-to-end energy conversion process dynamics is becoming critical because inertia-or synthetic inertia based approximated system analysis is generally invalid; the parameters derived in these models are at best valid when the system disturbances are small. This sets the basis for introducing energy as the main state variable.

Moreover, power conservation laws always must satisfy on the interfaces of components and/or sub-systems. This becomes a basis for selecting the rate of change of energy (or instantaneous real power in lossless case) as the state variable.

Finally, not all power produced can be delivered to where is needed. This is fundamentally due to the mismatch in rates at which energy conversion processes within the connected components take place; these non-thermal losses must be captured and are modeled by modeling reactive power dynamics, as derived earlier in this paper. This becomes the basis for reactive power as an interaction variable.

Modeling energy, power and rate of change of power as state variables makes it possible to abstract modeling of electric energy system dynamics to the level of spatial and/or temporal granularity (zooming in/zooming out) of interest without having to use different variables for different models. Design and operation of the rapidly changing electric energy systems require such unified models. In particular, protocols and standards are needed for integrating these highly distributed components/sub-systems so that their sub-objectives become as aligned as possible with the system-level objectives.

This modeling becomes a basis for cooperative control design to ensure that the interconnected system stability conditions and the inefficiencies are minimized, as will be reviewed in the next sub-section.

4.3 Notions of dynamic inefficiencies and interconnected system stability

It has been shown in [2] that the instantaneous reactive power characterizes the dynamic inefficiencies. From Eqn. (6), the rate of energy conversion of the component i results in a useful positive component delivered to the neighbors and certain wastage which does not get delivered and is lost due to unalignment of the phases of effort and flow variables that contribute to useful work. This relation can be expressed as follows.

$$p_i = \underbrace{\int_0^t 4E_{t,i}(\tau)d\tau}_{\text{Rate of change of useful work}} - \underbrace{Q(t)}_{\text{Rate of change of inefficiencies}} \tag{10}$$

Furthermore, by taking the integral of stored energy in tangent space as a storage function and instantaneous reactive power entering the sub-system as the supply function, it has been shown that the sub-system is dissipative for the chosen supply function, i.e. if and only if the rate at which real power injected into the system is less than the rate at which it gets dissipated. Mathematically,

$$\frac{d}{dt}\left(\int_0^t 4E_{t,i}(\tau)d\tau\right) \leq \dot{Q}_i \qquad \text{iff} \qquad \dot{P}_i \leq \frac{\dot{E}}{\tau_i} \tag{11}$$

This condition is fundamental and can be applied at any hierarchical level due to the simplicity of the modeling and the additivity of the variables in the energy space.

In the context of the grid in Fig. 1, stability and efficiency conditions derived can then be utilized to analyze system dynamics of interest, and to, consequently design cooperative control so that the system as a whole is stable and feasible. We close here by observing that generalizing ACE control to controlling dynamics of interactions between the areas and within the areas so that frequency is within the pre-specified standards, requires modeling dynamics of instantaneous reactive power and the dynamics of stored energy in tangent space. At the power rates relevant for solar PVs it becomes necessary to model these rates, as the steady-state ACE does not capture oscillations

caused by their very fast power changes. Moreover, since these deviations are no longer small, it is necessary to modernize the internal automation of diverse energy conversion processes so that they in the closed-loop can be characterized in terms of energy/power/rate of change of power. In the next section, we formalize the interactive multi-layered control for complex electric energy systems based on these observations.

5 Centralized optimal control formulation

It follows from the previous section that today's hierarchical control does not lend itself to the systematic operation of complex electric energy systems. This is mainly because many assumptions embedded in the industry practice generally do not hold. This requires one to enhance today's operating standards and protocols to facilitate stable and efficient deployment and utilization of new resources. In this paper, we suggest that it is possible to enhance today's hierarchical control by establishing standards/protocols for performance objectives and the related interaction specifications in energy space. These are typically real power/rate of change of real power injected into an electric energy source and taken out by the load, respectively.

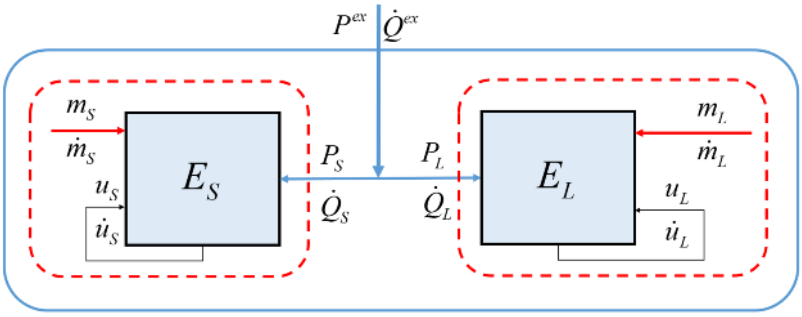

Fig. 4 Small system optimization in energy space

We introduce without loss of generality the basic formulation for such enhanced control using a small single source, single load system shown in Fig. 4. The source and load sub-systems have local exogenous disturbances characterized through $(m, \dot{m})$ and $(u, \dot{u})$ respectively, appended with subscript 'S' for source and 'L' for load. Since there is a physical limit on the rates at which the control input can vary, typically because of the physical limitations, the ranges of disturbance predictions and also ranges of its rate of change are required. In addition to the local disturbances, there may be an exogenous system-level disturbances characterized through the interactions $\left(P^{ex}, \dot{Q}^{ex}\right)$.

We first pose the continuous-time optimal control problem to identify the difficulties in solving this monolithic centralized problem. Next, we provide a brief overview of the importance of internal automation to convexify the input-output characteristics of the devices. This can then lead to straight-forward spatial and temporal decomposition of the benchmark problem formulation into more tangible sub-problems.

5.1 Centralized continuous time single layer optimization

The main objective of operating this system is to maximize physical efficiency in a feasible and stable way. Given the fact that temporal and spatial separation between today's tertiary, secondary and primary layers of control can no longer be assumed to hold, we start by posing the problem of efficient operations as a continuous-time dynamic problem first.

An enhanced provable performance version of today's hierarchical control is possible by posing the problem of supply-demand balancing at instantaneous time as a dynamic optimization of its efficiency subject to the dynamic interaction models (Eqns. (12e)-(12g)) coupled through the interconnection constraints (Eqns. (12b)-(12c)) and the dissipativity constraint (Eqn. (12d)). These models are further coupled to physical models through the definitions in (3) for obtaining initial conditions.

Input: Local Distrubances $m_i(t) \qquad \forall i \in \{S, L\}$

Exogenuous distrubances $P^{ex}(t)$

Problem to be solved:

$$\min_{\substack{u_i(t) \\ \forall i \in \{S,L\}}} \int_{t=0}^{H} \left(\dot{Q}_S^2(t) + \dot{Q}_L^2(t) \right) dt \tag{12a}$$

Interconnection constraints :

$$P_S(t) + P_L(t) + P^{ex}(t) = 0 \tag{12b}$$

$$\dot{Q}_S(t) + \dot{Q}_L(t) + \dot{Q}^{ex}(t) = 0 \tag{12c}$$

Dissipativity constraint :

$$\dot{P}^{ex}(t) \leq \frac{\dot{E}_S(t)}{\tau_S} + \frac{\dot{E}_L(t)}{\tau_L} \tag{12d}$$

Interaction dynamics :

$$\dot{E}_i(t) = P_i(t) - \frac{E_i(t)}{\tau_i} = p_i \tag{12e}$$

$$\dot{p}_i(t) = 4E_{t,i}(t) - \dot{Q}_i(t) \tag{12f}$$

$$\dot{E}_{t,i}(t) = P_{t,i}(t) - \frac{E_{t,i}(t)}{\tau_i} \qquad \forall i \in \{S, L\} \tag{12g}$$

Component physical constraints :

$$\dot{x}_i(t) = f_{x,i}\left(x_i(t), u_i(t), m_i(t), P_i(t), \dot{Q}_i(t)\right) \tag{12h}$$

$$y_i(t) = f_{y,i}\left(x_i(t), u_i(t), m_i(t), P_i(t)\right) \tag{12i}$$

$$u_i^{\min} \leq u_i(t) \leq u_i^{\max} \qquad \dot{u}_i^{\min} \leq \dot{u}_i(t) \leq \dot{u}_i^{\max} \tag{12j}$$

$$y_i^{\min} \leq y_i(t) \leq y_i^{\max} \qquad \dot{y}_i^{\min} \leq \dot{y}_i(t) \leq \dot{y}_i^{\max} \quad \forall i \in \{S, L\} \tag{12k}$$

This problem is solved for a pre-specified time of H. The internal detailed model is shown by the component-level physical constraints in Eqn. (12h)-(12k). Eqn. (12j) and (12k) model the control saturation limits and the permissible limits on outputs of interest, such as the currents through certain wires, voltages across certain equipment, internal temperature specifications of water heaters, etc. The energy space model, however, would require initial conditions using the knowledge of state variables at time $t = 0$ and invoking the relations in Eqn. (3).

Notice that the problem posed above can be solved for each instant of time in a decoupled way, had there been no time-coupling constraints. The problem above requires the time trajectory of the exogenous disturbances entering the system. In reality, perfect information of these signals is not available ahead-of-time. These signals can only be predicted over different timescales and the predictions become more accurate as we approach real-time. Also, the available control has certain physical limitations and so the problem above may not even have a feasible solution. As a result, slower resources might have to be activated ahead of time, in anticipation of low-frequency exogenous disturbances. The temporal alignment of available control with those of the available multi-rate predictions is essential to make the problem posed above feasible. Furthermore, for large-scale energy systems, the number of decision variables and constraints increase to the extent that the problem posed above quickly becomes intractable. In the sections to follow, we pose the temporally and spatially decoupled formulations for better addressing the respective complexities involved. Any of the decoupling across components is valid only if the internal model is convex as well.

Implied in this formulation is that the components can be characterized in terms of power/energy. For example, it is assumed that the system load consumes constant real/reactive power. Similarly, a controlled component, generator with its local automation, is assumed to be capable of controlling real power within its capacity limits. Instead, an implied assumption has been that the governor can stabilize frequency to the set point given by the droop and that the droop relation always holds. Neither of these is generally true, in particular when large relatively fast deviations in system load over time happen. An example of such net system deviation is the "duck curve" system load in California [101]. It has been only recently that such a controller for a

conventional synchronous generator was proposed [102]. A discussion on the primary control to convexify the complicated internal constraints next, followed by the resulting benchmark centralized problem formulation that will then be decomposed across multiple agents in Section 6.

In the sections to follow, the average quantities are defined for time-varying $x(t)$ over time $t \in [(k-1)T_t, kT_t]$ as

$$x[k] = \frac{1}{T_t} \int_{t=(k-1)T_T}^{t=kT_t} x(t)dt \tag{13}$$

5.2 Disturbance characterization

Another problem concerning solving this optimal control problem is temporal complexity. The time-trajectory of exogenous disturbances is not known ahead-of-time. They can only be predicted with certain levels of accuracy. For instance, the exogenous disturbances are decomposed two different ways as shown below

$$\begin{aligned} P^{ex}(t) &= P^{ex}(kT_t) + \Delta P^{ex}(t) \\ P^{ex}(t) &= \underbrace{P^{ex}(kT_t) + \Delta P^{ex}(nT_s)}_{P^{ex}(nT_s)} + \Delta P^{ex}(t) \end{aligned} \tag{14}$$

The first decomposition is used if only feed-forward control at T_t is desired while the second one is used when coordination is desired also at much faster T_s timescales. The remaining unpredictable changes $\Delta P^{ex}(t)$ manifests itself as the variations in interactions entering the components and are expected to be managed by the feedback controllers embedded in the components. Similar decomposition can be performed for the local disturbances as well. Here, $T_s << T_t$ and k, n respectively represent the sample number numbers associated with T_t and T_s-evolving predictions.

Remark 3 *The first predictable component $P(kT_t)$ can be made every T_t timestep. These can in addition be multi-rate. For instance, $P^{ex}(kT_t)$ can further be split into ones varying at multiple rates which are predictable as $P^{ex}(kT_t) = P^{ex}(k_1T_1) + P^{ex}(k_2T_2) + \ldots$ where $T_1 = 1$ hour for hour-ahead predictions, $T_2 = 15$ minutes for 15-minute-ahead predictions and for each of the rates k_1, k_2 represent the respective sample numbers. For simplicity, however, we only consider one feed-forward evolution rate in this section and postpone the discussion on handling multi-rate predictions to Section 7.*

Shown in Fig. 5 is one such load characterization. Generally as shown in the figure, the predictable component is available every T_t time interval and is represented with its sample number k as $P[k]$. At the same time, the variation during one T_t interval is represented using the bounds on the variation through

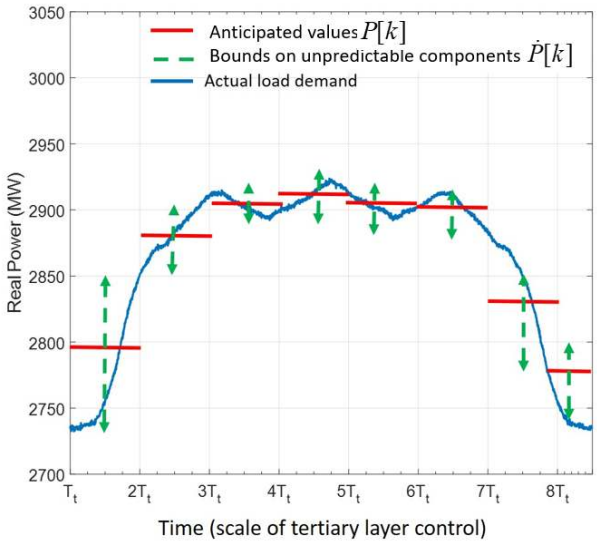

Fig. 5 Typical variation of inflexible demand at a substation: Red colored steps correspond to predictable components P[k] while the green color ones correspond to the range of variation, the worst case of which is represented as $\dot{P}[k]$

$\dot{P}[k]$ which can be modeled in two different ways depending on the available granularity of load predictions.

$$\dot{P}[k] = \frac{1}{T_t} \max_{t\in[(k-1)T_t, kT_t]} (P(t) - P[k]) \tag{15a}$$

$$\dot{P}[k] = \frac{1}{T_s} \max_{nT_s\in[(k-1)T_t, kT_t]} \Delta P[n] \tag{15b}$$

The first one is used if only maximum value during a time interval of T_t is known, while the second one can be used if more granular information is available. In Fig. 5 for instance, more granular measurements are not available and thus the first approach is utilized in the quantification of $\dot{P}[k]$.

Similar decomposition can be made use of, for the characterizing the local disturbances m_i seen by the components as well. Ideally, it is desired to have the following information,

$$\dot{P}[k] = \max_{t\in[(k-1)T_t, kT_t]} \dot{P}(t) \tag{16}$$

Since the derivative of real power is not available in practice, we rather utilize one of the approximations in Eqn. (15). Clearly, the second one out of the two more closely approximates the desired value of the maximum rate of change of real power. Furthermore, the second alternative is also better if very fast coordination of imbalances through AGC-type of control is desired at T_s rate.

Remark 4 *While having both P and Q is desirable to complete the space of interactions at each component, the quantification of $\dot{P}$ for procuring reserves is sufficient since the upper bound for both $\dot{P}(t)$ and $\dot{Q}(t)$ is $\dot{P}[k]$ as defined in Eqn.* (16) *and approximated through the available measurement using one of the Eqns. in Eqn.* (15).

$$|\dot{P}(t)| = \left| e_i \frac{df_i}{dt} + f_i \frac{de_i}{dt} \right| \leq \left| e_i \frac{df_i}{dt} \right| + \left| f_i \frac{de_i}{dt} \right| \approx \dot{P}[k] \tag{17a}$$

$$\left|\dot{Q}(t)\right| = \left| e_i \frac{df_i}{dt} - f_i \frac{de_i}{dt} \right| \leq \left| e_i \frac{df_i}{dt} \right| + \left| f_i \frac{de_i}{dt} \right| \approx \dot{P}[k] \tag{17b}$$

We introduce a vector new notation for the variables in energy space as

$$z_i = \begin{bmatrix} E_i \\ p_i \\ E_{t,i} \end{bmatrix} \qquad z_i^{in} = \begin{bmatrix} P_i \\ \dot{P}_i \\ \dot{Q}_i \end{bmatrix} \qquad z_i{}^{out} = \begin{bmatrix} P_i^{out} \\ \dot{P}_i^{out} \\ \dot{Q}_i^{out} \end{bmatrix}$$

Remark 5 *It is only when the interaction dynamics settle that we have $z_i^{\text{in}}(t) = z_i^{\text{out}}(t)$.*

5.3 Stabilization and regulation of interaction variables

Notice that the problem posed in Eqns. (12) has possibly only the constraints in Eqn. (12h) - (12i) to be non-linear and/or non-convex. This results in the possibility of having multiple solutions which imply that none of the decomposition strategies in the literature can be put to use. The internal physical dynamics can be as detailed as desired to model certain phenomena that are to be monitored and/or controlled. Ultimately from the system perspective, however, only the interactions matter. Thus, we propose to first design internal control to convexify these constraints while ensuring internal stability over longer timescales. By doing so, over longer timescales, the decomposition of the problem posed above across multiple agents will remain valid. This does not necessarily imply that the optimal solution for instantaneous time can be achieved. It is only in an average sense over kT_t interval that we achieve an optimal solution.

The unpredictable continuous time-evolving component $\Delta m_i(t)$ can further be decomposed into slower and faster-evolving sub-components each of which may be handled by different available local control actions [103]. For the exposition of concepts, we assume only one rate evolution of this hard-to-predict component of the disturbance. After having designed such stabilizing control in energy space, the relations over T_s time interval can be established as in (18a), thereby abstracting the inner complicated dynamical models [102, 104].

$$\begin{aligned} y_i[n] - y_i[n-1] = \alpha_i^P[k]\left(P_i[n] - P_i[n-1]\right) + \alpha_i^Q[k]\left(\dot{Q}_i[n] - \dot{Q}_i[n-1]\right) \\ +\alpha_i^m[k]\left(m_i[n] - m_i[n-1]\right) + \alpha_i^u[k]\left(u_i[n] - u_i[n-1]\right) \end{aligned}$$

Here, the constants $\alpha_i^P, \alpha_i^Q, \alpha_i^m, \alpha_i^u$ are the droop coefficients of the component i implementable by the feedback control $\forall(k,n) s.t. nT_s \in [(k-1)T_t, kT_t]$.

However, the droop characterization over T_s rates leads to convexification. In a simple form, this droop relation is written as

$$\Delta y_i[n] = F_{D,i}^u \Delta u_i[n] + F_{D,i}^m \Delta m_i[n] + F_{D,i}^P \Delta P_i[n] + F_{D,i}^Q \Delta \dot{Q}_i[n] \tag{18a}$$

Here the matrices $F_{D,i}^u, F_{D,i}^m, F_{D,i}^P, F_{D,i}^Q$ characterize the closed-loop sensitivity of the output variables with respect to controllable inputs, disturbances and grid interactions respectively. The values of $\Delta P_i[n], \Delta \dot{Q}_i[n]$ as a result of interactions with neighbors can not be known accurately enough. As a result, the bounds on variation quantified through $\dot{P}[k]$ can rather be utilized for obtaining worst-case deviations in output variables of interest as it plans for the control evolution locally.

The validity of the above droop model is also subject to the limits on the interactions with the rest of the system. The droop relation above, along with the limits on outputs of interest, disturbances, and controllable inputs, can be utilized to obtain limits on the grid power interactions. With such a characterization to replace the internal model of the component in Eqn. (12), it is possible to obtain a unique equilibrium owing to quadratic costs and linear constraints.

In summary, the primary control of the component is thus supposed to serve three objectives.

- To stabilize the internal dynamics for all values of interactions in this range
- To convexify the models dictating the evolution of outputs of interest in the closed-loop
- To find the range of interactions that will be feasible and stable for the component in closed-loop

Serving these three objectives is a complex task. Systematic design for such primary control of interaction variables is currently work in progress. Much of the nonlinear control proposed such as feedback linearizing control of synchronous machines; field-oriented control of induction machines; energy-based control of wind power plants, energy-based inverter control of batteries and solar PVs can be shown to be based on using rate of change of power or acceleration as variables to control. As a rule, they are not capable of maintaining terminal voltage close to nominal because of the assumptions made when deriving these controllers. It has been only recently shown that nonlinear controllers for both real power and rate of change of reactive power while minimizing deviations in voltage from the nominal, have been introduced [105]. For some examples of nonlinear control design for ensuring real power and rate of change of real power, see [106–108]. A detailed discussion of such nonlinear controllers is beyond the scope of this paper. Instead of having centralized coordination for ensuring stability and feasibility as system conditions change, it will be shown how to have an interactive self-adjusting stabilization protocol in energy space in the rest of the paper.

5.4 Discrete-time centralized formulation

By applying the feedback control, the quasi-static droop relations in Eqn. (18a) along with limits on interaction variables can be utilized to replace the internal constraints (Eqns. (12h) - (12k)) in the centralized optimal control problem posed. Furthermore, by utilizing the definitions of the average quantities in (13), the centralized continuous-time problem posed in Eqn. (12) can be converted to a discrete-time problem shown below.

Input: Multi-rate predictions of local distrubances $m_i[k], m_i[n] \quad \forall i \in \{S, L\}$

Predictable component of exogenuous distrubances $P^{ex}[k]$

Maximum rate of change of its deviaiton $\dot{P}^{ex}[k]$

Problem to be solved:

$$\min_{\substack{z_i^{in}[k],\, u_i[n] \\ \forall i \in \{S,L\}}} \sum_{kT_t=0}^{kT_t=H} \left(\dot{Q}_S[k]^2 + \dot{Q}_L[k]^2 \right) \tag{19a}$$

Interconnection constraints :

$$\begin{aligned} P_S[k] + P_L[k] + P^{ex}[k] &= 0 \\ \dot{Q}_S[k] + \dot{Q}_L[k] + \dot{Q}^{ex}[k] &= 0 \\ \dot{P}_S[k] + \dot{P}_L[k] &\geq \dot{P}^{ex}[k] \end{aligned} \tag{19b}$$

Dissipativity constraint :

$$\dot{P}^{ex}[k] \leq \frac{p_S[k]}{\tau_S} + \frac{p_L[k]}{\tau_L} \tag{19c}$$

Interaction Dynamics :

$$\begin{aligned} E_i[k] &= E_i[k-1] + T_t \left(P_i[k] - \tfrac{E_i[k]}{\tau_i} \right) = E_i[k-1] + T_t p_i[k] \\ p_i[k] &= p_i[k-1] + T_t \left(4E_{t,i}[k] - \dot{Q}_i[k] \right) \\ E_{t,i}[k] &= E_{t,i}[k-1] + T_t \left(\left(\tfrac{P_i[k] - P_i[k-1]}{T_t} - \dot{P}_i[k] \right) - \tfrac{E_{t,i}[k]}{\tau_i} \right) \end{aligned} \tag{19d}$$

Time coupling :

$$\begin{aligned} P_i[n] &= P_i[k] + \Delta P_i[n] & \dot{Q}_i[n] &= \dot{Q}_i[k] + \Delta \dot{Q}_i[n] \\ \left| \tfrac{\Delta P_i[n]}{T_s} \right| &\leq \dot{P}_i[k] & \left| \Delta \dot{Q}_i[n] \right| &\leq \dot{P}_i[k] \end{aligned} \tag{19e}$$

Internal physical constraints :

$$\begin{aligned} y_i[n] = y_i[n-1] &+ F_{D,i}^u \left(u_i[n] - u_i[n-1] \right) + F_{D,i}^m \left(m_i[n] - m_i[n-1] \right) \\ &+ F_{D,i}^P \left(P_i[n] - P_i[n-1] \right) + F_{D,i}^Q \left(\dot{Q}_i[n] - \dot{Q}_i[n-1] \right) \end{aligned}$$

$$\begin{aligned} {u_i}^{\min} \leq u_i[n] \leq {u_i}^{\max} \qquad & \dot{u}_i^{\min} \leq \tfrac{u_i[n] - u_i[n-1]}{T_s} \leq \dot{u}_i^{\max} \\ {y_i}^{\min} \leq y_i[n] \leq {y_i}^{\max} \qquad & \dot{y}_i^{\min} \leq \tfrac{y_i[n] - y_i[n-1]}{T_s} \leq \dot{y}_i^{\max} \\ \forall (n,k) | nT_s \in [(k-1)\, T_t, kT_t] \qquad & \forall i \in \{S, L\} \end{aligned} \tag{19f}$$

In the problem posed in Eqn. (19), the integral in (12a) is converted to that in (19a) by pre-multiplying the objective by $\frac{1}{T_t}$ followed by splitting the integral and by applying the definition of average quantities in (13). The constraints in Eqn. (12e)-(12g) are all pre-multiplied by $\frac{1}{T_t}$ and an integral operator is applied for time varying in the interval $t \in [(k-1)T_t, kT_t]$. Notice that additional interconnection constraint for the rates of changes of real power was required to ensure there is enough flexibility from the controllable resources to handle hard-to-predict deviations within the T_t interval. The maximum rates of variations of controllable components are coupled with the faster evolving T_s signals in the internal constraints in Eqn. (19f) through Eqn. (19e). Notice also that since the rates of deviation of both instantaneous real and reactive power are bounded above by $\dot{P}[k]$ as pointed out in Remark 4, we can have the same upper bound for both P and $\dot{Q}$ variation over T_s scale in Eqn. (19e). It must be understood that $\dot{Q}[k]$ is approximately equal to $\omega Q[k]$ as computed in the case of periodic signals. This signal only changes slowly as ω varies. However, other deviations because the signals are time-varying are better captured through $\Delta\dot{Q}[n]$.

Remark 6 *It may appear that the decision variable $\dot{P}_i[k]$ does not have an upper limit. Notice however that the value of $P_i[k]$ and $P_i[k-1]$ depends on the values the exogenous disturbances, through the constraints in Eqn.* (19b)*. Both of these values dictate the value of $\dot{P}_i[k]$ since the value of $E_{t,i}$ is typically close to zero for all T_t as the local feedback control stabilizes the internal dynamics.*

Clearly, the above posed problem is convex because of the quadratic cost functions and the linear constraints in terms of $z_i[k]$, $z_i^{in}[k]$, $z_i^{in}[n]$, $y_i[n]$ and $u_i[n]$. Thus, if the problem above is feasible there exists a global optimum in the average sense over T_t interval. Notice that the problem formulation is for the two-component models for the exposition of concepts, but in reality, there may be thousands of components forming a network, thereby increasing the number of decision variables and constraints proportionally. As a result, the problem becomes intractable. Furthermore, typically, the internal droop coefficients are a function of internal control design, which the agents may not be willing to share. Because of this, we propose a novel interactive formulation based on a primal-dual decomposition strategy for obtaining the solution of the problem posed in Eqn. (19), so that the computation is tractable for large systems, while also protecting sensitive local information. This will be described in Section 6.

5.5 Variants of conventional power flow equations

The problem posed in Eqn. (19) is a generalization of the ACOPF and DCOPF formulations currently used in operations and markets. To see this, we derive the network model used in ACOPF from the general interaction dynamics. If the dynamics of interactions of the wires are assumed to be instantaneous, the Eqns. (12e)-(12g) written for the wire can be used to obtain the relations:

$$P_i = \frac{E_i}{\tau_i} \tag{20a}$$

$$\dot{Q}_i = 4E_{t.i} \tag{20b}$$

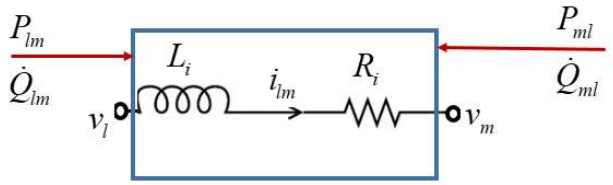

Fig. 6 Power flows into an RL model of the wire i between the nodes l and m of the power system network

This equation can be simplified by substituting the expression in terms of periodic voltage and current signals at each of the nodes as $v_l = |V_l| sin(\omega t + \theta_l)$ concisely written as $\text{Re}(|V_l|\angle\theta_l)$[1] and similarly for node m. Let the resistance and inductance of the wire i be denoted as R_i and L_i respectively.

In the following derivation of traditionally utilized ACOPF equations, we assume that the voltage and current signals are both square integreable (belong to $L2$ function space), and they are periodic w.r.t time T i.e. $v(t+T) = v, i(t+T) = i$. Let us define the inner product for this Hilbert space as $\langle a(t)|b(t)\rangle = \frac{1}{T}\int_0^T a(t)b(t)dt$. If the decomposition of these signals is possible into multiple frequency components where the magnitudes of each of the frequency signals are all collected in vectors A, B respectively, the inner product can also be written as $\langle A, B\rangle$ where this inner product is defined on euclidean space. We can now simplify the first equation in Eqn. (20) as

$$P_{lm}{}^{\text{OPF}} + P_{ml}{}^{\text{OPF}} = P_i{}^{\text{OPF}} = \frac{1}{T}\int_0^T P_i(t)dt = \frac{1}{T}\int_0^T \frac{E_i(t)}{\tau_i}dt \tag{21a}$$

$$= \frac{1}{T}\int_0^T (R_i x_i)x_i dt \tag{21b}$$

$$= \frac{1}{T}\int_0^T \left(v_l - v_m - L_i\frac{di_{lm}}{dt}\right) i_{lm} dt \tag{21c}$$

$$= \left\langle \left(v_l - v_m - L_i\frac{di}{dt}\right)|i_{lm}\right\rangle \tag{21d}$$

$$\Rightarrow P_{lm}{}^{\text{OPF}} + P_{ml}{}^{\text{OPF}} = (V_l - V_m)^T I_{lm} \tag{21e}$$

$$= (V_l - V_m)^T (V_l - V_m)(G_i - jB_i) \tag{21f}$$

$$= \text{Re}\left(\begin{pmatrix} -|V_l||V_m|\angle(\theta_l - \theta_m) \\ -|V_l||V_m|\angle(\theta_m - \theta_l) \\ +|V_l|^2 + |V_m{}^2| \end{pmatrix}(G_i - jB_i)\right) \tag{21g}$$

[1] $|V|\angle\theta$ is a short hand for complex phasor domain representation of the signal $|V|cos(\omega t + \theta) + j|V|sin(\omega t + \theta)$ where V is the amplitude of the signal, ω is the carrier frequency, θ is the voltage phase angle and $j = \sqrt{-1}$

In the Eqn. (21a), $D_i(x_i) = \frac{E_i}{\tau_i}$ is the damping of the comopnent which is defined as the integrand shown in Eqn. (21b) [2]. is substituted where D_i is the damping matrix of the element [2]. The wire, being a two-port component, the expression for P_i in the interaction model is substituted with the net interaction represented as the sum of power flows from both the ports. The state variable of the wire is the current through the inductor, it can be substituted in place of x_i. Eqn. (21c) follows from the application of Kirchoff's voltage law. Eqn. (21d) is derived by utilizing the fact that for periodic signals, the inner product of the signal and its derivative is always equal to zero which can be proven through the space vector decomposition of the signal [109]. Next, in Eqn. (21e) we expand the space vector decomposed signals of v_l, v_m, i_{lm} denoted using vector V_l, V_m, I_{lm} to obtain inner products in the Euclidean space. In Eqn. (21f), we substitute the constitutive relation of I_{lm} where $G_i - jB_i = \frac{1}{R_i + jX_i}$ is the admittance of the component. Finally, the vectors representation can be written in the complex domain as shown in Eqn. (21g) which matches the one obtained in standard power flow equations [1, 6, 11].

Next, we derive the expression for reactive power similarly. It was shown in [93] that the phasor domain modeling results in the instantaneous reactive power rate to be equal to the product of carrier frequency and the phasor domain reactive power traditionally utilized in the analysis of power grids.

$$\frac{1}{T}\int_0^T \dot{Q}_i(t)dt = \omega\left({Q_{lm}}^{\text{OPF}} + {Q_{ml}}^{\text{OPF}}\right) \tag{22}$$

We can simplify the expression for $\dot{Q}_i$ as:

$$\frac{1}{T}\int_0^T \dot{Q}_i(t)dt = \frac{1}{T}\int_0^T 4E_{t,i}(t)dt = \frac{1}{T}\int_0^T 2\left(L_i\dot{x}_i\right)\dot{x}_i dt \tag{23a}$$

$$= \frac{2}{T}\int_0^T \left(v_l - v_m - R_i i_{lm}\right)\frac{di_{lm}}{dt} \tag{23b}$$

$$= 2j\omega(V_l - V_m)^T(I_{lm}) \tag{23c}$$

$$= 2j\omega(V_l - V_m)^T(V_l - V_m)\left(G_i - jB_i\right) \tag{23d}$$

$$\Rightarrow (Q_{il} + Q_{im}) = -\text{Im}\left(\begin{pmatrix} -|V_l||V_m|\angle(\theta_l - \theta_m) \\ -|V_l||V_m|\angle(\theta_m - \theta_l) \\ +|V_l|^2 + |{V_m}^2| \end{pmatrix}\left(G_i - jB_i\right)\right) \tag{23e}$$

Here, the definition of $E_{t,i}$ as in Eqn. (3) for this wire, is substituted in Eqn. (23a). Since x_i here represents current, the integrand is the voltage drop across inductor. Invoking Kirchoff's voltage laws, we obtain the expression in Eqn. (23b). By applying the space vector decomposition and also since the space vector decomposed signals of i_{lm} and $\frac{di_{lm}}{dt}$ are orthogonal to each other, we obtain the expression in Eqn. (23c). This vector product which when written in complex domain results in the final expression in Eqn. (23e).

In summary, we see that the energy space modeled equations we derived for instantaneous time, for modeling interactions and their dynamics across

transmission line are general relations, from which the ACOPF equations can be derived under static phasor domain modeled signals assumption.

Furthermore, when the voltage magnitude is assumed to phase angles can be avoided and if $R_i << X_i$, one can obtain the decoupled ACOPF equations:

$$\begin{aligned} P_{lm} + P_{ml} = 0 = \left(\tfrac{|V_l||V_m|}{X_i}\sin(\theta_l - \theta_m)\right) + \left(\tfrac{|V_m||V_l|}{X_i}\sin(\theta_m - \theta_l)\right) \\ Q_{lm} + Q_{ml} = -2\tfrac{|V_l||V_m|}{X_i}\cos(\theta_l - \theta_m) = -\left(\tfrac{|V_l||V_m|}{X_i}\cos(\theta_l - \theta_m)\right) \\ -\left(\tfrac{|V_m||V_l|}{X_i}\cos(\theta_m - \theta_l)\right) \end{aligned} \tag{24}$$

When the angle difference is very small and the voltage magnitude is assumed to be unity, the above equations can be simplified to obtain real power flow relations only, referred to as DCOPF equations given as

$$P_{lm} + P_{ml} = 0 = \left(\frac{1}{X_i}(\theta_l - \theta_m)\right) + \left(\frac{1}{X_i}(\theta_m - \theta_l)\right) \tag{25}$$

Note that the cost function utilized in OPF or economic dispatch models is the cost of generators which can also be considered in our formulation in addition to physical inefficiency minimization. Furthermore, the inter-temporal constraints are typically considered only in the economic dispatch formulations with DCOPF equation in today's operations. These constraints model the flexibility of the generation devices alone through an empirically constructed ramp rates, which may or may not be implemented by the physical automation on the generator reacting to the frequency and/or voltage deviations. Also, our formulations comprise of the interconnected system dissipativity condition which assures that the optimum operating point is stable for the given set of disturbances entering the grid [2].

6 DyMonDS-based interactive method for resource management

It is evident from the problem formulation in Eqn. (19) that this problem can not be solved all at once by a single entity. In order to make the problem tractable, decomposition across hierarchical agents is desired. The literature has traditionally utilized primal and/or dual decomposition-based iterative approaches to solve such problems. Instead, we propose an interactive method to solve the problem in Eqn. (19) efficiently.

In this method, we have two types of problems, one solved by the components/iBAs and the other solved by the higher-level optimizers (aggregators, ISOs, markets). The lower layers compute bid functions characterizing the sensitivity of their optimal solution with respect to price. The objective of the higher-level optimizers is to optimize the device bids to find the best values of interactions from the range specified by the iBAs so that their higher-layer objectives are met. Their decision-making problems are posed in terms of the same common variables as those by which the lower-layer specifications are characterized. In this sense, the resulting protocol is a win-win protocol, since

all entities operate within the ranges of common interaction variable values they have mutually agreed upon. This avoids the problem of difficult interfacing of heterogeneous multi-physical components.

Remark 7 *If it is not possible to find a feasible solution for given specifications, the higher-layer optimizing entities need to plan for new equipment/technologies (storage, for example) to be added to the system.*

Both problems are solved simultaneously until pre-specified convergence criteria are satisfied. The information exchange from the iBAs to the coordinators is in the form of sensitivity functions, rather than the point-wise solution. This solution strategy considerably reduces the number of iterations, as will be described later in the section.

Furthermore, the proposed modeling in energy space lends itself naturally to supporting both biddings by the lower layers (components, sub-systems) and to the system-level market clearing and pricing. It also provides a theoretical foundation for defining the type of information exchange required to incentivize provision and consumption of the right market derivatives.

Remark 8 *Notably, instead of characterizing derivatives in terms of QoS attributes (frequency and voltage), all derivatives are defined in general energy space over the stratum of triplet products comprising specifications of power, rate of power and rate of reactive power in a feed-forward manner over several temporal market time horizons T_i, $i \in 1, 2, 3 \ldots$. This derivative provided in a feed-forward way for specific time horizon T_i is*

$$(Market \;\; Derivative)_{T_i} = \left[(P)\,;\left(\dot{P}\right);\left(\dot{Q}\right)\right]_{T_i} = \left[z^{in}\right]_{T_i} \tag{26}$$

Each of the market derivatives is further associated with a price

$$(Price)_{T_i} = \left[\left(\lambda^{P}\right);\left(\lambda^{\dot{P}}\right);\left(\lambda^{Q}\right)\right]_{T_i} = [\lambda]_{T_i} \tag{27}$$

In this section, we focus on single rate market derivatives utilization for the proposed decomposition strategy. But this is however generalizable to multi-rate derivative and in fact, acts as a driver to the extent of risk taken by the entities. This is explained in detail in Section 7.

6.1 Master problem solved by market coordinator

As described previously, For a specific timescale T_t, we now pose the problem that is to be solved by the market operator. The system-level coupling constraints in Eqn. (28) (i.e. Eqn. (28b)- Eqn. (28c)) are all accounted for, as the bids from the lower layers are optimized. These bids are supposed to abstract all the rest of the constraints in Eqn. (19e)-Eqn. (19f) in the centralized benchmark problem posed.

Input: Predictable component of exogenuous distrubances $P^{ex}[k]$

Maximum rate of change of its deviation $\dot{P}^{ex}[k]$

Bids for real, reactive power and their rates $B_i^z(z_i^{in}[k])$

Ranges of controllable interactions $z_i^{out,\min}[k], z_i^{out,\max}[k]$

Problem to be solved:

$$\min_{\substack{z_i^{in}[k] \\ \forall i \in \{S,L\}}} \sum_{i\in\{S,L\}} \sum_{kT_t=0}^{kT_t=H} \underbrace{\left(\dot{Q}_i[k]^2\right)}_{\text{Inefficiencies}} + \underbrace{B_i^z\left(z_i{}^{in}[k]\right)}_{\text{Component preferences}} \tag{28a}$$

Interconnection constraints :

$$\begin{aligned} &P_S[k] + P_L[k] + P^{ex}[k] = 0 && \left(\lambda^P[k]\right) \\ &\dot{Q}_S[k] + \dot{Q}_L[k] + \dot{Q}^{ex}[k] = 0 && \left(\lambda^Q[k]\right) \\ &\dot{P}_S[k] + \dot{Q}_L[k] \geq \dot{P}^{ex}[k] && \left(\lambda^{\dot{P}}[k]\right) \end{aligned} \tag{28b}$$

Dissipativity constraint :

$$\dot{P}^{ex}[k] \leq \frac{p_S[k]}{\tau_S} + \frac{p_L[k]}{\tau_L} \qquad \left(\mu^E[k]\right) \tag{28c}$$

Interaction Dynamics :

$$\begin{aligned} &E_i[k] = E_i[k-1] + T_t\left(P_i[k] - \tfrac{E_i[k]}{\tau_i}\right) = E_i[k-1] + T_t p_i[k] \\ &p_i[k] = p_i[k-1] + T_t\left(4E_{t,i}[k] - \dot{Q}_i[k]\right) \\ &E_{t,i}[k] = E_{t,i}[k-1] + T_t\left(\left(\tfrac{P_i[k]-P_i[k-1]}{T_t} - \dot{P}_i[k]\right) - \tfrac{E_{t,i}[k]}{\tau_i}\right) \end{aligned} \tag{28d}$$

Device Preferences :

$$z_i{}^{out,\min}[k] \leq z_i[k] \leq z_i{}^{out,\max}[k] \tag{28e}$$

Each of the coupling constraints is now associated with Lagrange multipliers $\lambda^P[k], \lambda^Q[k]$ and $\lambda^{\dot{P}}[k]$ for real, reactive power balance and flexibility. We thus have defined these quantities as market derivatives. The dissipativity constraint in Eqn. (28c) also is a coupling constraint and its lagrange multiplier is associated with a linear combination of the energy and power, i.e. $\mu^E[k]$ is associated with the quantity $P_i[k] - \frac{E_i[k]}{\tau_i}$. Market derivatives do not exist for stability yet and it is thus assumed that this inequality constraint is not binding at optimality in this draft. The way this market product can be put to use for the future possibility of inclusion of stability-related market products is described briefly in Section 8.

The objective function comprises the inefficiencies modeled previously. But in addition, there are device price elasticities or bid functions denoted by $B_i^z(z_i) = B_i^P(P_i) + B_i^{\dot{P}}\left(\dot{P}_i\right) + B_i^Q(\dot{Q}_i)$, where each of the terms corresponds to bid functions for each of the marker derivatives. These functions indicate the willingness to provide services through each of the market derivatives. In addition, the permissible values of these market derivatives i.e. $z_i^{out,\min} =$

$\left[P_i^{\min}[k], \dot{P}_i^{\min}[k]\dot{Q}_i^{\min}[k]\right]^T$ and $z_i^{out,\max} = \left[P_i^{\max}[k], \dot{P}_i^{\max}[k]\dot{Q}_i^{\max}[k]\right]^T$ are also submitted as a part of the bid function, which are operating conditions dependent.

Remark 9 *Notice that the limits submitted along with bid functions by the iBAs/component are that of z_i^{out} defined in Eqn.* (9) *and computed using the relations in Eqn.* (18a). *The input interactions, however, are the result of the clearing mechanism by the coordinator. By sending the limits of z_i^{out} to the coordinator, so that z_i^{in} is within these limits, the component, can implement such schedules to make $z_i^{in} = z_i^{out}$ while stabilizing the dynamics as it responds to local disturbances at instantaneous time.*

The second component of input and output interactions further provide information on how much of the net disturbances may enter the component due to the unpredictability of both local and exogenous disturbances. Sufficient reserves, therefore, are set aside for such operating conditions within the time interval T_t which get implemented through a feedback mechanism. The feedback also gets implemented through control gains that are based on cleared prices, which may be such that the fastest and slowest components get scheduled according to their need. As a result, the feedback mechanism can manage such hard-to-predict disturbances by having planned properly for the ranges of these values and their variations.

6.2 Agent-level problem

The bid functions to be utilized by the coordinator need to be computed given the values of the prices associated with each of the market derivatives i.e. given the estimates $\hat{\lambda}[k]$ the agent i solves the optimization sub-problem which can be stated as shown in Eqn. (29).

Input : Price predictions for interactions:$\hat{\lambda}_i[k]$

Multi-rate predictions of local distrubances $m_i[k], m_i[n]$

Problem to be solved:

$$\min_{u_i[n], z_i^{in}[k]} \sum_{kT_t=0}^{H} \left(\underbrace{\left(\sum_{nT_S=(k-1)T_t}^{nT_S=kT_t} \dot{Q}_i[n]^2 \right)}_{\text{Local Inefficiencies}} \underbrace{\begin{array}{l} -\hat{\lambda}^P[k]P_i[k] - \\ \hat{\lambda}^Q[k]\dot{Q}_i[k] - \hat{\lambda}^{\dot{P}}\dot{P}_i[k] \end{array}}_{\text{Revenues/Bills}} \right) \tag{29a}$$

Time coupling :

$$\begin{array}{ll} P_i[n] = P_i[k] + \Delta P_i[n] & \dot{Q}_i[n] = \dot{Q}_i[k] + \Delta\dot{Q}_i[n] \\ \left|\frac{\Delta P_i[n]}{T_s}\right| \leq \dot{P}_i[k] & \left|\Delta\dot{Q}_i[n]\right| \leq \dot{P}_i[k] \end{array} \tag{29b}$$

Internal physical constraints :

$$
\begin{aligned}
y_i[n] &= y_i[n-1] + F^u_{D,i}\left(u_i[n]-u_i[n-1]\right) + F^m_{D,i}\left(m_i[n]-m_i[n-1]\right) \\
&\quad + F^P_{D,i}\left(P_i[n]-P_i[n-1]\right) + F^Q_{D,i}\left(\dot{Q}_i[n]-\dot{Q}_i[n-1]\right) \\
{u_i}^{\min} &\le u_i[n] \le {u_i}^{\max} \qquad \dot{u}_i^{\min} \le \tfrac{u_i[n]-u_i[n-1]}{T_s} \le \dot{u}_i^{\max} \\
{y_i}^{\min} &\le y_i[n] \le {y_i}^{\max} \qquad \dot{y}_i^{\min} \le \tfrac{y_i[n]-y_i[n-1]}{T_s} \le \dot{y}_i^{\max}
\end{aligned} \tag{29c}
$$

While the component is supposed to satisfy all the local constraints, the objective is to minimize the local inefficiencies while also making revenues from the markets. Furthermore, the agent is supposed to ensure the contractual commitments over kT_t are met. The latter is modeled as a hard constraint through Eqn. (29b). This can, however, be relaxed, depending on the penalties imposed by the operator if the commitments aren't fulfilled. The problem above which when solved for perturbations in $\lambda^P[k]$ lets one capture the cost sensitivity w.r.t real power injection. This is integrated to form the bid functions for real power injection $B_i^P(P_i)$ and similarly for the reactive power injection as $B_i^Q(\dot{Q}_i)$ and that for flexibility $B_i^{\dot{P}}[k]$.

The limits on y_i, u_i and ranges of disturbances and their rates can now be converted to those on a function of P_i and Q_i from the droop relation in Eqn. (18a) by simply applying a projection operator. It must be noted that this approach is very different from convex relaxations typically utilized in convexifying the network constraints. This relaxation is exact only for radial networks [37]. In our approach, however, the projection operator is such that the ranges of interaction variables found will be valid for any feasible region of the internal variables. For each interaction variable value, there may exist multiple possible values of internal variables, if the projection operator is rank deficient, which often is the case. The result of this optimization by the source is a bid function for the market derivative characterized by the limits on the market derivatives and the corresponding price elasticities or bid functions $\left\{B_i^P(P_i), B_i^Q(\dot{Q}_i), B_i^{\dot{P}}(\dot{P}_i)\right\}_{T_t}$ over a market time-interval T_t.

These bid functions are now utilized by the system operator to solve the problem posed in Eqn. (28) to obtain new prices and quantities, which are now utilized to recompute the bid functions at the components. This process is repeated until the successive values of cleared prices and quantities converge.

Remark 10 *Notably, if the price predictions are accurate, single iteration of exchange of bids with the coordinator results in obtaining an optimal solution. This is theoretically proven in Appendix A.1.*

Shown in Fig. 7 is the basic information exchange required between the lower-level market participants and the coordinating market-clearing layer. It is extremely important to observe that this interactive information exchange results in the same centralized optimum in continuous time. This result is a direct consequence of the fact that this is a linear quadratic convex optimization problem and the interactive design is simply an implementation of the dual decomposition. It differs from the traditional approach of decomposition tech-

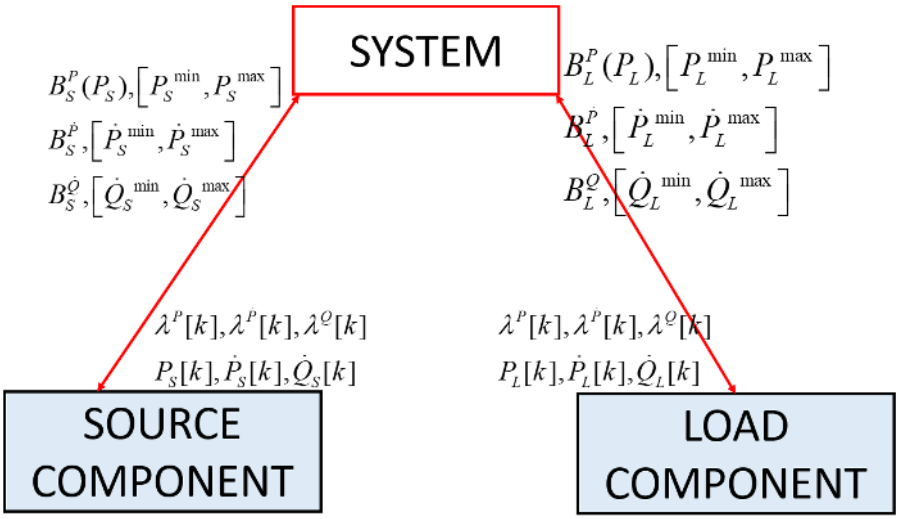

Fig. 7 Multi-layered implementation of electric energy markets

niques because of interactive formulations employing bid functions computed as a function, instead of the point-wise bids.

Remark 11 *Mapping back the optimum interaction specifications* $z_i^{\text{in},*}[k] = \left[P_i^*[k], \dot{P}_i^*[k], \dot{Q}_i^*[k]\right]$ *back to the control input that needs to be applied may be non-unique. A unique solution* $u_i[n]$ *can be obtained only if the matrix* $F_{D,i}^u$ *in Eqn.* (18a) *is invertible. Alternatively, this value can be uniquely determined if the objective function in Eqn.* (29) *also includes the cost of control effort, and then re-solve Eqn,* (29) *for given value of* $P_i[k] = P_i^*[k]$ *and* $\dot{Q}_i[k] = \dot{Q}_i^*[k]$ *to ensure reproducibility of the solutions* $u_i[n]$ *that has to be applied with an objective to manage faster varying local disturbances* $m_i[n]$.

It should be noted that at very fast timescales, the local control action is assumed to cancel the effect of fast time-varying disturbances $\Delta m_i(t)$ and a component $\Delta P^{ex}(t)$ manifesting itself as $\Delta P_i(t)$ at the component i. In fact, it has been shown in [110] that the feedback reacting to the reactive power at the interfaces leads to the disturbance rejection at these fast timescales. This may seem to be competitive in nature and may be sub-optimal, but we conjecture that this may be near-optimal if the local feedback control gain scheduling is done utilizing the cleared price information every T_t interval.

Remark 12 *It should be noted that at very fast timescales, the local control action is assumed to cancel the effect of fast time-varying disturbances* $\Delta m_i(t)$ *and a component* $\Delta P^{ex}(t)$ *manifesting itself as* $\Delta P_i(t)$ *at the component* i. *It has been shown in [110] that the feedback reacting to the reactive power at the interfaces leads to the disturbance rejection at these fast timescales. This may seem to be competitive and may be sub-optimal, but we conjecture that*

this may be near-optimal if the local feedback control gain scheduling is done utilizing the cleared price information every T_t interval.

6.3 DyMonDS-based fast primal-dual approach with minimal coordination

The distributed agents in the previous sub-sections may not, however, have enough intelligence to accurately predict the prices. If they start with an estimate of these prices, the iterative information exchange of the bids, cleared quantities and prices between the coordinator and the agents needs to be performed until convergence. The bid function sensitivities can also be computed using the following expression, instead of performing sensitivity analysis [111]. This is particularly useful when the local constraints are inequality constraints and/or are too restrictive. In this section, we use the shorthand z_i in place of z_i^{in}

$$\frac{\partial B_i^z}{\partial z_i^k} = \underbrace{\left(\nabla^2_{z_i} f_i(z_i^{k-1})\right)}_{a_i^k} z_i^k + \underbrace{\left(\nabla_{z_i} f_i(z_i^{k-1}) + H_i(x_i^{k-1}, z_i^{k-1}) - \nabla^2_{z_i} f_i(z_i^{k-1}) z_i^{k-1}\right)}_{b_i^k} \tag{30}$$

Here $H_i(x_i^{k-1}, z_i^{k-1})$ denotes the sub-gradient of the indicator function of all the constraints of the agent i, where x_i^{k-1}, z_i^{k-1} represents the solutions of internal variables and that of interactions z_i^{in} at $(k-1)^{th}$ iteration obtained by solving the agent-level problem for given values of prices at the $(k-1)^{th}$ iteration. $f_i(z_i)$ is the objective function of the agent-level problem, which is assumed to be doubly differentiable with respect to each of the components of z_i^{in}. By substituting the values of x_i^{k-1}, z_i^{k-1} into the analytical expression above, we obtain the bid functions for each of the market derivatives by integrating the expression w.r.t each of the components of z_i^k separately.

This method is concisely described by the Algorithm 1

In this algorithm, the agents/iBAs belong to a set $\mathcal{C}$ and assume some initial prices for each of the market derivatives. These values are utilized to solve the agent-level problem posed in Eqn. (29). This problem is solved to obtain a temporary solution that is utilized to compute sensitivity coefficients a_i^k and b_i^k. In the computations of b_i^k, the sub-gradient of the indicator function $H_i(x_i, z_i)$ is equal to zero since (x_i, z_i) belong to the constraint set of component i. Also, the tolerable values of these interaction variables are computed by projecting the feasible space of internal variables and interaction variables onto the interaction space by utilizing the constraints in Eqn. (29c).

These bid functions are now such that they capture the marginal cost preferences of the agents while satisfying internal constraints. These functions which when utilized to clear the bids subject to the coupling constraints, results in another iterate of cleared quantities and prices. These get utilized by the agents to solve their own problem once again to compute bid functions. This process repeats until pre-specified convergence criteria is met. The convergence proof of this iterative method is shown in Appendix B.

Algorithm 1: DyMonDS-based algorithm at time step mT_t

Initialization: For each component $i \in \mathcal{C}$, select $z_i^0[m] = z_i[m-1]$ for time sample $m > 1$ else set randomly
For each node $j \in \mathcal{N}$, select $\lambda_j^0[m] = \lambda[m-1]$ for $m > 1$ else set randomly
Step k: For the iteration count $k \geq 1$, execute following steps until convergence
(A) **Component-level computations:**
(A.1) **Bid creation** For each agent $i \in \mathcal{C}$
$(x_i, z_i) \leftarrow$ Solve Eqn. (29) given $z_i^k[m], \lambda^k[m]$

$$a_i^k = \nabla_{z_i}^2 f_i(z_i) \tag{31}$$

$$b_i^k = \left(\nabla_{z_i} f_i(z_i) + H_i(x_i, z_i) - \nabla_{z_i}^2 f_i(z_i) z_i\right) \tag{32}$$

$$B_i^k(z_i) = \frac{1}{2} a_i^k {z_i}^2 + b_i^k z_i \tag{33}$$

(A.2) **Limits computation:**
$\left(z_i^{k,out,\min}[m], z_i^{k,out,\max}[m]\right) \leftarrow$ Use Eqn. (18a) and Eqn. (29c)
(B) **Clearing of price and quantities by the coordinator:**
$\left(z_i^{k+1}[m], \lambda_j^{k+1}[m]\right) \leftarrow$ Solve Eqn. (28) given $B^k(z_i), z_i^{k,out,\min}[m], z_i^{k,out,\max}[m]$

Remark 13 *Notice that the sensitivity functions computed are a quadratic approximation of the iBA's cost functions and the internal constraints. Hence, at the coordination stage, the KKT constraints look similar to that of the optimality conditions of the second order approximation of Taylor's theorem, which is the basis of several variants of proximal gradient methods. In fact, if the initial guess is within the region of convergence, a single iteration is enough. This is so because the modeling framework itself results in linear constraints with quadratic costs with strong convexity. This is however not often the case since the quadratic bid functions are computed by each component around certain assumed values of Lagrange multipliers, that correspond to initial guess of the solution vector. These values keep getting better and in fact the numerical tests indeed suggest that it only takes a couple of iterations to reach a near-optimal point, which is sufficiently accurate for large systems (See Appendix).*

7 DyMonDS-based interactive risk management

The power grid is always vulnerable to unforeseen events, which might be low-impact or high-impact ones, that can force complete grid shut down. It is important to quantify the impacts and have well-designed protocols for risk mitigation planning. These risks can be associated with long-term high-impact events such as loss of generators or a wire, or it can even be a shortage of ramping capability of the generators that fail to offset the sudden large changes in the inflexible power injections/consumptions into/from the grid. With the deregulation in electricity markets, the reserves for reliability are also traded for. These market products may lead to high-profit margins for the generators, but at the same time, this may mean that the generator is

being under-utilized and may thus lead to inefficient operation and/or even loss of revenues. Typically the capacity set aside is compensated for through lost opportunity costs in the markets, but this may still, however, lead to the less efficient operation of the components and grid as a whole. With the advent of Intent of Things, aggregates of small devices are also capable of providing such reserves at an aggregate level. This however again is associated with risks at the component-level, aggregator/iBA-level and also at the system coordinator level.

The objective ultimately is to make sure there is no scarcity of resources in the future for unanticipated changes in the grid power injections. The operator may not feel the need to procured reserves for some unforeseen event which may only occur with less than 0.1% probability. But with this, the operator is leaving the grid vulnerable possibly to a large portion of load shed. The cost overhead involved in reliable operation of grid versus the risk associated with not taking any preventive actions due to concerns of efficient operation should be weighed against one another through unified metrics, to better manage the risks associated. Unified metrics in terms of energy and power shed, flexibility availability, etc, can be measured straightforwardly at any of the hierarchical levels and also in times of need, can ensure suitable control strategies to be implemented in short time. In particular, we propose to utilize our modeling framework supported with DyMonDS-based primal-dual solution strategy to risk assessment and management.

For operations, a lot of uncertainty stems from the unpredictability of the future load. As a result, each of the grid entities faces risk. DyMonDS approach enables distributed entities to weigh their risks according to their own preferences. We show three possible approaches through which the end-users and/or system coordinator can make an informed choice, considering all the risks associated with load uncertainty manifesting as price uncertainty.

- Approach 1: Embedded model predictive control in the iBAs to produce energy bids; static clearing of energy alone by the system coordinator
- Approach 2: Stratum of multi-temporal markets for clearing energy products only
- Approach 3: Multiple market products
- Approach 4: Stratum of multi-temporal markets for clearing both energy and reserve products

For each of the approaches, the cleared prices cam uniquely be found and thus the pros and cons of each of the approaches for different grid entities can be assessed in detail.

7.1 Approach 1: Embedded model predictive control in the iBAs to produce energy bids & static clearing of energy alone by the system coordinator

Through the embedded model predictive control at the agents, price predictions and local disturbance evolutions for the future intervals are predicted so

that the present time interval bidding is made in response to its anticipated future profits or losses and/or energy scarcity that the grid may experience.

At any time instant, by neglecting the effect of local constraints, the bid created by the agent at the present time instant is a function of future prices as follows

$$\frac{\partial B_i[k]}{\partial z_i} = \sum_{kT_t \in [t,t+H]} \frac{\partial C_i[k]}{\partial z_i} + \sum_{k^+T_t \in [t+kT_t,t+H]} \hat{\lambda}[k^+] \tag{34}$$

Here the second term is a result of the anticipated prices of energy in the future. For higher future prices for instance, the generator can allocate resources for future by planning the path for the time instants before accordingly. As a result, the actual prices at the instant when scarcity arises can be eliminated, thus resulting in uniform prices. Typically, the price spikes indicate inefficiencies in the markets. With the embedded MPC, these spikes can be eradicated.

7.2 Approach 2: Stratum of multi-temporal markets for clearing energy products only

This has been a long-standing good practice in the electric power industry and has been instrumental to efficient dispatch of resources. We refer here to this practice as the horizontal dispatch, which effectively means that the slowest resources, such as the nuclear and coal power plants, are turned on and dispatched to supply long-term base load; then closer to real-time somewhat faster units, gas and oil power plants, are turned on, and the output of slower units is adjusted only if necessary. This practice is qualitatively different from what one may refer to as the vertical dispatch which requires all power plants to be re-dispatched in a feed-forward way day-ahead market (DAM), and adjusted in the real-time market (RTM). The major challenge here is whether local automation actually can implement the commitments made during bidding.

Assuming the local control is provable, our proposed modeling framework also facilitates the functioning of multiple markets in a provable manner largely because of the linearity of the coupled formulations. The trade-offs analysis can typically be made at the bid creation stage, perhaps by considering the inter-temporal costs involved in longer-term markets through the terminal costs in the shorter term bidding. Such methods have been referred to as hierarchical MPC and has been pursued in [112, 113]. Another approach to ensuring multiple markets at the coordination stage alone can be referred to in [114].

7.3 Approach 3: Embedded MPC in iBAs to produce energy and reserve bids & static co-optimization of energy and reserves by the system coordinator

In Section 6, we have already discussed the implications of having to utilize the rate of change of real power as a market derivative to ensures enough reserves

are available. These can be traded for at different timescales to ensure enough ramp capability is available at different rates. However, the present approaches do not provide a proper signal to value the flexibility of the resources thus restricting the adoption of advanced control strategies and/or technology mix.

Having multiple market products for instance for voltage and frequency is seemingly a weak signal. This is because the one-one mapping of the cause and effect can not be shown explicitly with the markets set up for the control of these physical variables. On the other hand, we propose that the mismatch in frequency and/or voltage is a result of energy imbalances at respective timescales. These imbalances in terms of energy and power create a much stronger signal which can be associated with the risk assessment metrics and take preventive actions accordingly.

7.4 Approach 4: Stratum of multi-temporal markets for clearing both energy and reserve products

A combination of all the above approaches to handling the risk can be combined, wherein market participants bid their utility functions for different time horizons and different market derivatives. The qualitative difference shows up in market outcomes because of inherent uncertainties. These include system load uncertainties, uncertain equipment status and deviations of bid implementations from the commitments. To discuss these in some detail, consider without loss of generality a stratum of feed-forward markets clearing the following market derivatives: (1) DAM and RTM energy clearing $T[k_h]$ for $h \in \{1, 2, \dots 24\}$, and $T[k_m]$ for $m \in [h-1, h]$, respectively; (2) DAM and RTM ancillary service clearing $T[k_h]$ for $h \in \{1, 2, \dots 24\}$, and $T[k_m]$ for $m \in [h-1, h]$, respectively; and, (3) DAM and RTM reliability clearing $T[k_h]$ for $h \in \{1, 2, \dots 24\}$, and $T[k_m]$ for $m \in [h-1, h]$, respectively. While these derivatives are clearing at the same feed-forward time horizon, their basic functionalities are different. The energy market is intended to balance predictable components of supply and demand; ancillary service market provides bounds on power corresponding to hard-to-predict load deviations during normal equipment conditions, so that frequency is regulated within the time intervals for which the commitment is made. Finally, the reliability market derivative is needed to support electric energy service during extreme conditions such as forced equipment outages. While energy market design is somewhat standardized, the ancillary service and reliability markets are at best work in progress. In short, there exist major disconnects between the operating standards, and the market incentives needed to support electricity service as the industry evolves. Explaining these problems is much beyond the objectives of this paper. Instead, we have only shown that conceptualization of how one could align operating standards and market design in the energy space is possible.

8 Future research

8.1 Potential to ensure stable markets

At the time this paper is written, much has changed both in state-of-the-art nonlinear distributed control design and the power-electronically-switched hardware for their implementation. The emerging electric energy systems could become much more controllable for provable performance without requiring excessive fast communications. In particular, delivery system components, controllable load, renewable resources, fast storage can all contribute to an end-to-end performance, instead of having to burden excessively large conventional generators. It has been documented well in the literature that one can avoid wear-and-tear of mechanically controlled governors by relying on power electronically controlled other types of equipment, fast storage, in particular. Notably, instead of having constant gain PID controllers, it is essential to have more adaptive nonlinear controllers capable of stabilizing and regulating faster and larger, often non-zero-mean fluctuations. These can be combined with distributed model-predictive controllers capable of smoothing out the effects of fast power fluctuations on frequency and voltage.

Most recently, there has been an influx of literature regarding the possibility of controlling frequency and voltage by these new power electronically switched, inverter controlled, unconventional resources. Missing is a formalized standard/protocol for integrating these fast controlling new resources into the existing system with clear specifications needed to support electric energy market implementation stably and reliably. Not negligible, there is a need to provide incentives to these technologies to do so at well-understood economic value. If this were to be included as a market product, the objective function in Eqn. (28a) can be replaced with the following:

$$\min_{u_i[n]} \sum_{kT_t=0}^{H} \left(\begin{array}{l} \underbrace{\sum_{nT_S=(k-1)T_t}^{nT_S=kT_t} \left(\left(\dot{Q}_i[n] \right)^2 \right)}_{\text{Local inefficiences}} \underbrace{\begin{array}{l} -\hat{\lambda}^P[k] P_i[k] \\ -\hat{\lambda}^Q[k] \dot{Q}_i[k] - \hat{\lambda}^{\dot{P}}[k] \dot{P}_i[k] \end{array}}_{\text{Revenues/Bills}} \\ \qquad \underbrace{-\hat{\mu}^E[k] \left(\frac{1}{\tau_i} \left(P_i[k] - \frac{E_i[k]}{\tau_i} \right) \right)}_{\text{Revenues for stabilizing the grid}} \end{array} \right) \tag{35}$$

Given today's industry standards for fast control of generators, it is possible to enhance these standards so that they in a unified technology-agnostic way support stable response of the system and market clearing processes. The basic idea is to have local automation embedded into many diverse resources (supply, demand, delivery) which provide their conditions-dependent specifications about their ability to stabilize their response. To seamlessly integrate market signals with the complex local automation design, it is necessary to specify their performance in terms of triplet input-output specification about energy market derivative associated with market time horizon T_i as described in Section 6.

8.2 Cyber-secure operation

It follows from these modeling and optimization formulations that operating future electric energy systems efficiently and reliably only requires multi-layered information exchange of interaction variables. This further defines critical information for ensuring cyber-secure operation. Instead of having to monitor data-congested flows, this modeling defines what matters, at specific temporal and spatial granularity. This results in having cyber-secure methods in support of manageable information flow within an otherwise extremely complex dynamical network. The modeling framework aligns technical, economic and cyber-security objectives when pursuing next-generation SCADA. Even very advanced methods for cyber-secure software coding become implementable [115]. While this paper sets the main framework at the conceptual level, it at the same time opens the possibility for designing advanced software algorithms, including reinforcement learning and approximate dynamic programming for enabling cyber-secure operations.

9 Next Steps

This paper introduces basic principles for enhancing SCADA used by today's electric power industry. The dichotomy of requiring higher temporal and spatial data granularity, on one hand, and the complexity of managing such data, on the other, is overcome by proposing modeling for optimization and control in energy space. The approach is fundamentally modular in which different zoomed-in/zoomed-out temporal and spatial system representations are characterized using interaction variables. These are triplets of power, rate of power and rate of reactive power. As such, they are technology agnostic and not dependent on specific energy conversion processing internal to the modules. This modeling is used to formulate enhanced hierarchical control for these systems. It is shown that in the energy space, system-level dynamic optimization is fundamentally a convex dynamic optimization problem. As such, it lends itself to primal-dual decompositions and can serve as the basis for protocols in future electric energy systems.

Notably, the approach is an outgrowth of today's area control error (ACE) concept used in automatic generation control (AGC). While AGC is expected to regulate the frequency of AC electrical power systems in response to small slow power imbalances, the interaction variables used in this paper is a triplet of power, rate of power and rate of reactive power, and it can be defined for any spatial and temporal granularity. This generalization is essential for operating electric energy systems which are vertically disintegrated (multiple ownership objectives) and have generally stochastic highly varying inputs. Protocols for communicating and controlling these variations can and should be designed using future generation SCADA, we refer to as DyMonDS. Efforts are under the way to work with industry.

Acknowledgements This material is based upon work supported by the Department of Energy under Air Force Contract No. FA8721-05-C-0002 and/or FA8702-15-D-0001. Any opinions, findings, conclusions or recommendations expressed in this material are those of the authors and do not necessarily reflect the views of the Department of Energy.

Appendix

A Theoretical basis for the provability of DyMonDS-based bids

Let us first pose the problem for allocation of resources in general form. From the benchmark problem described in Eqn. (19), one can see that the coupling constraints are all linear in interaction space. Let us use the notation $z_i[k]$ to represent interactions including $E_i, p_i, P_i, \dot{Q}_i$ for all time samples $kT_t \in [t, t+H]$. The internal variables of including $x_i[k], u_i[k], m_i[k]$ for the same time samples are all abstracted in the vector x_i (with slight abuse of notation). Let x, z denote the vectors x_i, z_i for all components stacked up.

The centralized problem can then be posed in a general form as shown below:

$$\begin{aligned} (C): \quad & \min_{z_i} \sum_{i \in \mathcal{N}} f_i(z_i) \\ s.t. \quad & \\ & g(z) \leq 0 \qquad (\lambda) \\ & h_i(x_i, z_i) \leq 0 \qquad (\mu_i) \end{aligned} \tag{36}$$

The first constraint function $g(z)$ is a coupling constraint while the second one $h_i(x_i, z_i)$ is specific to each agent i. Solving the problem in Eqn. (36) turns out to be complicated since the number of components given by $|\mathcal{N}|$ is extremely large. While the coupling constraints given by $g(z)$ are linear, the number of internal constraints modeled through h_i for each agent i can be high, leading to a large-scale problem to be solved at once.

In this general formulation and the proofs to follow, a few assumptions are made:

Assumption 1 *The cost function $f_i : \mathbb{R}^{n_i} \to \mathbb{R}$ is a smooth convex function which is continuously differentiable with Lipschitz continuous gradients $L(f_i) > 0$ given as*

$$\|\nabla f_i(x_i) - \nabla f_i(y_i)\| \leq L(f_i) \|x_i - y_i\| \qquad \forall x_i, y_i \in \mathbb{R}^{n_i} \tag{37}$$

where $\|.\|$ denotes the standard Euclidean norm.

Assumption 2 *The constraint set given in (36) is a closed convex set.*

Exploiting the linearity of the coupling constraints, we have proposed a distributed approach towards solving the problem (C). As explained in Section 6, we propose to have the system operator solve the master problem comprising the coupling constraints alone which are of the same order as the number of nodes in the network. The increased cardinality of the problem created by local constraints and their preferences are rather abstracted through bid functions as computed by solving the agent-level problem in Eqn. (38)

$$\begin{aligned} (Agent - i): \quad & \min_{x_i, z_i} C_i(z_i) + \lambda_j^T g_j(z_i) \\ & s.t. \\ & h_i(x_i, z_i) \leq 0 \end{aligned} \tag{38}$$

Here, λ_j corresponds to the vector of all the elements of vector λ for which there exists dependence of the constraint on the elements of z_i i.e. $j \in \mathcal{J}$ to denote constraint indexes to which z_i contributes.

By solving the problem $(Agent - i)$ for perturbations in each of the elements in λ_j, one can obtain the bid functions $B_i^j(z_i)$ for use by the operator to solve the system level problem. The willingness of the agent to participate depends on its internal constraints but

also on the price incentive. The bid is such that it makes marginally the same amount of cost as it gets paid through the respective λ_j. As a result,

$$\frac{\partial B_i^j}{\partial z_i} = -\lambda_j = a_i^j z_i + b_i^j \tag{39}$$

The coefficients a_i^j and b_i^j are computed empirically by obtaining the points z_i by solving $(Agent - i)$ for slight perturbations in λ. This function is integrated with respect to z_i to obtain

$$B_i(z_i) = \sum_{j \in \mathcal{J}} B_i^j(z_i) = \frac{1}{2} z_i^T a_i z_i + b_i z_i \tag{40}$$

Here, $a_i = \sum_{j \in \mathcal{J}} a_i^j$ and $b_i = \sum_{j \in \mathcal{J}} b_i^j$. Along with the bid functions, the feasibility region of the agent i is projected onto the z_i plane represented by the space Π_i. This projected space varies with time as operating conditions change. This plane is found by utilizing the constraints Eqn. (19f). These bid functions along with the time varying limits of the feasible region of interaction variables are all collected by the system operator to solve the following problem:

$$\begin{aligned} &(S): \min_{z_i} \sum_{i \in \mathcal{N}} B_i(z_i) \\ &s.t. \\ &\qquad g(z) \leq 0 \qquad (\lambda) \\ &\qquad z_i \in \Pi_{g,i} \end{aligned} \tag{41}$$

Assumption 3 *The problem (C) is solvable and there exists a unique minimizer x^*.*

Notice that the projected space Π_i is also convex since the projection map is a linear operator, the constraint set of problem (S) is convex. Since the bid functions are by construction convex, there would be a unique minimizer of (S). We next prove that the optimal point obtained by the proposed distributed scheme is the same as the one obtained by the centralized approach.

A.1 Proof for approaching the centralized solution optimum operating point through proposed primal-dual decomposition strategy

Theorem 1 *Under assumptions 1-2, the solution obtained by solving (S) results in the same solution as that of the (C) when the bids $B_i(z_i)$ are created by solving problem in $(Agent - i)$ in response to small perturbations around $\lambda = \lambda^*$ where λ^* is the dual solution of the problem (C).*

Proof 1 *Writing the KKT conditions for the problem (C), we obtain:*
Stationarity:

$$\nabla_{z_i} C_i(z_i) + \lambda^T \nabla_{z_i} g(z) + \mu_i^T \nabla_{z_i} h_i(z_i, x_i) = 0 \qquad \forall i \in \mathcal{N} \tag{42a}$$

$$\mu_i^T \nabla_{x_i} h_i(z_i, x_i) = 0 \tag{42b}$$

Primal feasibility:

$$g(z) \leq 0 \tag{42c}$$

$$h_i(x_i, z_i) \leq 0 \tag{42d}$$

Dual feasibility:

$$\lambda \geq 0 \tag{42e}$$

$$\mu_i \geq 0 \quad \forall i \in \mathcal{N} \tag{42f}$$

Complementarity slackness:

$$\lambda^T g(z) = 0 \tag{42g}$$

$$\mu_i^T h_i(x_i, z_i) = 0 \quad \forall i \in \mathcal{N} \tag{42h}$$

Let the solution of above set of equations be $x_i^*, z_i^*, \lambda^*, \mu_i^*$.

Now, solving the problem posed in $(Agent - i)$ *for a given value of* λ*, we obtain the solution of the agent-level problem. As explained previously, the bid function is constructed by integrating the empirically constructed sensitivity given by*

$$\lambda(z_i) = -\nabla_{z_i} B_i(z_i) = a_i z_i + b_i \tag{43}$$

This results in the bid function $B_i(z_i) = \frac{1}{2} a_i z_i^2 + b_i z_i$.

Analytically, one can write the KKT conditions of the problem $(Agent - i)$ *to notice that the gradient of the bid function satisfies the following relation:*

$$-\nabla_{z_i} B_i(z_i) \nabla_{z_i} g(z) + \nabla_{z_i} C_i(z_i) + \lambda^T \nabla_{z_i} h(x_i, z_i) = 0 \tag{44a}$$

while also satisfying the device-specific KKT conditions given by the set S_i *i.e.*

$$S_i = \{(x_i, z_i, \lambda_i, \mu_i) \,|(42b), (42d); (42f); (42h)\} \tag{44b}$$

The set above which when projected onto the space of the z_i *plane results in* $z_i \in \Pi_{g,i}$*, representing the space of projection of the half space represented by* $g_i(x_i, z_i)$ *onto the* z_i *plane in order to commit operating conditions dependent limits of* z_i *as a part of the bid function. Clearly,* $z_i \in \Pi_i \implies (x_i, z_i, \lambda_i, \mu_i) \in S_i$ *for some values of* x_i, λ_i, μ_i.

Now considering these bid functions and the projected constraint on z_i *in the problem* (S)*. The KKT conditions of* (S)*can be written as:*
Stationarity:

$$\nabla B_i(z_i) + \lambda^T \nabla_{z_i} g(z_i) \qquad \forall i \tag{45a}$$

Primal, dual feasibility and complementary slackness:
Eqns. (42c), (42e), (42g)
An added constraint of the bid function that z_i *belongs to the projections of the set* S_i *ensures the other internal KKT constraints in Eqn.* (36) *remain feasible. Upon substituting the relations in Eqn.* (44) *into the stationarity condition in Eqn.* (45a) *for each agent* i *and summing them up, one could obtain the KKT conditions in Eqn.* (42)*. Thus proved.*

Remark 14 *When the internal constraints* g_i, h_i *are non-convex, multiple agent-level solutions may exist and thus centralized and distributed solutions may not be the same.*

B Proof for the rate of convergence of the DyMonDS-based sensitivity bids

B.1 Agent-level bid function

Following the definitions and proof sketch in [116], we now analyse the convergence rates for the proposed approach. First, we define the indicator function for the constraint set of the problem $(Agent - i)$ as $H_i(x_i, z_i)$. With this, we obtain a function to be minimized at the agent-level as

$$F_i(x_i, z_i, \lambda_j) = f_i(x_i, z_i) + H_i(x_i, z_i) + \lambda_j^T g_j(z_i) \tag{46}$$

Here, it is assumed that each agent's cost function is strongly convex, smooth and differentiable with a Lipschitz constant $L_i(f_i)$.

Definition 1 *The quadratic approximation of $F_i(x_i, z_i, \lambda)$ around the point y_i for $L_i \geq L_i(f_i)$ is given as*

$$Q_{L,i}(x_i, z_i, \lambda_j) = f_i(x_i, y_i, \lambda_j) + \langle z_i - y_i, \nabla_{z_i} f_i(x_i, y_i, \lambda)\rangle + \frac{L_i}{2}\|z_i - y_i\|_2^2 + H_i(x_i, z_i) + \lambda_j^T g_j(z_i) \tag{47}$$

It admits a unique minimizer

$$p_{L,i}(x_i, y_i, \lambda_j) = \arg\min_{z_i} Q_{L,i}(x_i, z_i, \lambda_j) \tag{48}$$

By denoting z_i as the minimizer and by using the notation $\gamma_i(x_i, y_i,) \in \frac{\partial H_i}{\partial z_i}(x_i, z_i)$, the optimality condition can be obtained from Eqn. (48) by taking the partial derivative w.r.t z_i and equating to zero.

$$\nabla_{z_i} f_i(x_i, y_i) + L_i(z_i - y_i) + \gamma_i(x_i, y_i) + \lambda_j^T \frac{\partial g_j}{\partial z_i} = 0 \tag{49}$$

Since the coupling constraints are linear, the partial derivative $\frac{\partial g_j}{\partial z_i}$ is a constant matrix. As explained previously, the marginal bid function at the agent level is equal to the expression for λ_j, for which the analytical expression can be decomposed into a slope a_i and intercept value b_i

$$\frac{\partial B_i^j}{\partial z_i} = -\lambda_j = \underbrace{\left(\frac{\partial g_j}{\partial z_i}\right)^\dagger L_i}_{a_i^j} z_i + \underbrace{\left(\frac{\partial g_j}{\partial z_i}\right)^\dagger (\nabla_z f_i(x_i, y_i) + \gamma_i(x_i, y_i) - L y_i)}_{b_i^j} \tag{50}$$

Here, $(.)^\dagger$ represents the pseudo inverse operation. The bid function then can be re-expressed as

$$B_i(z_i) = \sum_{j \in \mathcal{J}} B_i^j(z_i) = \frac{1}{2} z_i^T a_i(y_i) z_i + b_i(y_i) z_i \tag{51}$$

By collecting these bid functions from all the agents, the system cost function is constructed as

$$f^s(z) = \sum_{i \in \mathcal{N}} = \frac{1}{2} z_i^T a_i(y_i) z_i + b_i(y_i)^T z_i \tag{52}$$

Remark 15 *Notice that the system-lvel cost function is convex by construction. At each of the agents, the respective quadratic functions constructed, approximate the variation of their cost and the internal constraints around y.*

B.2 System-level optimality conditions

Similarly, defining the function $F^s(z)$ for the problem to be solved by the system operator as

$$F^s(z^k) = f^s(z^k, z^{k-1}) + G(z^k) \tag{53}$$

where $G(z^k)$ represents the indicator function of the coupling constraints $g(z^k) \leq 0$. We have $Q^s(z^k, y)$ to denote the quadratic approximation $F^s(z^k)$ around a point y for some $L^s > 0$ Around an arbitrary point y, the cost function coefficients are computed using the initial guess z^0.

$$Q^s(z^k, y^k) = f^s(z^k, z^{k-1}) + \left\langle z^k - y, \nabla_z f^s(y, z^0)\right\rangle + \frac{L^s}{2}\|z^k - y^k\|^2 + G(z^k) \tag{54}$$

The unique minimizer of the quadratic approximation of $F^s(z^k)$ around a point y is denoted as $p_L^s(y)$. The optimality conditions can explicitly be written as

$$\nabla_z f^s(y, z^0) + L^s\left(z^k - y\right) + \gamma^s(y) = 0 \tag{55}$$

Let us now define the sequence $\{z^k\}$ given by $z^k = p_L^s(z^{k-1})$

Remark 16 *The series $F^s\left(z^k\right)$ is contracting.*
Notice that $F^s(z^k) \leq Q^s\left(z^k, z^{k-1}\right) \leq Q^s\left(z^{k-1}, z^{k-1}\right) = F^s(z^{k-1})$

We will now derive its convergence rate.

B.3 Convergence proof

We begin by revising one of the lemmas in [116] for the distributed setting here, which will be utilized in the rest of our convergence proof:

Lemma 1 *For some $L^s > 0$ and $y \in \mathbb{R}^{n_z}$ if $F^s\left(p_L^s\left(y\right)\right) \leq Q_L^s\left(p_L^s\left(y\right), y\right)$. Then, $\forall z \in \mathbb{R}^{n_z}$,*

$$F^s(z^k) - F^s\left(p_L^s\left(y\right)\right) \geq \frac{L^s}{2}\|p_L^s(y) - y\|^2 + L^s\left\langle y - z^k, p_L^s(y) - y\right\rangle \tag{56}$$

Proof 2 *Notice that the condition in Lemma holds true if $L^s = L_y^s = diag(a_i(y_i))$ i.e. the matrix created by the quadratic coefficient of the bid function. Because of the convexity of f^s with respect to z^k and since G is an indicator function of the convex set of coupling constraints, we can establish the following relations:*

$$f^s(z^k, z^{k-1}) \geq f^s(y, z^0) + \left\langle z^k - y, \nabla f^s(y, z^0)\right\rangle \tag{57}$$

$$g(z^k) \geq g(p_L^s(y)) + \left\langle z^k - p_L^s(y), \gamma(y)\right\rangle \tag{58}$$

We can now write the expression for the objective function as

$$F^s(z^k) \geq f^s(y, z^0) + \left\langle z^k - y, \nabla f^s(y, z^0)\right\rangle + g(p_L(y)) + \left\langle z^k - p_L(y), \gamma(y)\right\rangle \tag{59}$$

Furthermore, from the definition of Q, we have

$$Q(p_L(y), y) = f^s(y, y^0) + \left\langle p_L(y) - y, \nabla f^s(y, z^0)\right\rangle + \frac{L^s}{2}\|p_L(y) - y\|^2 + g(p_L(y)) \tag{60}$$

Subtracting the two equations, we obtain

$$F^s(z^k) - Q(p_L(y), y) \geq \left\langle z^k - p_L(y^k), \nabla f^s(y, z^0) + \gamma(y)\right\rangle - \frac{L^s}{2}\|p_L(y) - y\|^2 \tag{61}$$

Utilizing the assumption stated in the lemma and substituting the optimality condition in Eqn. (55) in the right hand side, we obtain

$$F^s(z^k) - F^s(p_L(y)) \geq L\left\langle z^k - p_L(y^k), z^k - y\right\rangle - \frac{L^s}{2}\|p_L(y) - y\|^2 \tag{62}$$

$$= \frac{L^s}{2}\|p_L(y) - y\|^2 + L^s\left\langle y - z^k, p_L(y) - y\right\rangle \tag{63}$$

Theorem 2 *Let $\{z^k\}$ denote the series produced by the update rule $z^k = p_L^s\left(z^{k-1}\right)$. Then, the system-level objective function converges at the rate of $\mathcal{O}\left(1/k\right)$ as follows:*

$$F^s\left(z^k\right) - F^s\left(z^*\right) \leq \frac{\|z^0 - z^*\|_{L0}}{2k} \tag{64}$$

where z^* is the optimal point and L_0 is the diagonal matrix consisting of the quadratic coefficients of the bid functions of each of the agents.

Proof 3 *Invoking the Lemma 1 with* $z^k = z^*, y = z^n, L^s = L_n = diag(a_i(z_i^n))$, *we have*

$$\begin{aligned} F^s(z^*) - F^s\left(z^{n+1}\right) &\geq \tfrac{L_n}{2}\left(\|z^{n+1} - z^n\|^2 + 2L_n\left\langle z^n - z^*, z^{n+1} - z^n\right\rangle\right) \\ &= \tfrac{L_n}{2}\left(\|z^* - z^{n+1}\|^2 - \|z^* - z^n\|^2\right) \\ &= \tfrac{1}{2}\left(\|z^* - z^{n+1}\|_{L_n}^2 - \|z^* - z^n\|_{L_n}^2\right) \end{aligned} \tag{65}$$

Next, invoking the Lemma 1 with $z^k = z^n, y = z^n, L^s = L_n = diag(a_i(z_i^n))$, *we have*

$$F^s(z^n) - F^s\left(z^{n+1}\right) \geq \frac{1}{2}\|z^{n+1} - z^n\|^2{}_{L_n} \tag{66}$$

Summing the inequality in Eqn. (65) *over* $n = 0, 1, \ldots k-1$, *we have*

$$kF^s(z^*) - \sum_{n=0}^{k-1} F^s\left(z^{n+1}\right) \geq \|z^* - z^k\|_{L_{k-1}}^2 - \|z^* - z^0\|_{L_0}^2 \tag{67}$$

Next, multiplying the inequality in Eqn. (66) *by* n *and summing the result over* $n = 0, 1, , \ldots k-1$, *we have*

$$-kF^s(z^k) + \sum_{n=0}^{k-1} F^s\left(z^{n+1}\right) \geq \sum_{n=0}^{k-1} n\|z^{n+1} - z^0\|_{L_n}^2 \tag{68}$$

Now, by adding equations (67) *and* (68), *we obtain*

$$F^s\left(z^k\right) - F^s\left(z^*\right) \leq \frac{\|z^* - z^0\|_{L0}}{2k} \tag{69}$$

Here, the cleared values at each iteration are communicated to the agents which are utilized to compute the new bid functions. As a result, at k^{th} iteration, the bids are computed using the solution obtain by system coordinator at $(k-1)^{th}$ iteration. The system level objective function convergence stated above indicates that these bid functions converge at a rate of $\mathcal{O}(1/k)$.

Note also that error at each iteration is because of the quadratic approximation of the bid function by the agents. The error in the This result combined with the existence of unique solution as obtained by the centralized and distributed solution strategies as shown in Theorem 1 ensures that the DyMonDS approach leads to the centralized optimal solution.

Remark 17 *The computational complexity through this approach of minimal coordination is of the order* $\mathcal{O}\left(n_z^3\right) + \sum_{i=1}^{|\mathcal{N}|}\mathcal{O}\left(n_{x_i}^3\right)$, *where* $n_z, n_{x,i}$ *respectively represent the number of interaction variables, and number of state variables in each of the components of the network. Typically* n_{x_i} *for each* i *is much smaller than* n_z *of the entire system.*

The centralized solution complexity would be of the order $\mathcal{O}\left(\left(n_z + \sum_{i=1}^{|\mathcal{N}|} n_{x_i}\right)^3\right)!$

In order to compare with iterative approaches such as ADMM, simple update equations are typically utilized in addition to solving the local agent problems with a computational cost of $\sum_{i=1}^{|\mathcal{N}|}\mathcal{O}\left(n_{x_i}^3\right)$. *However, the number of iterations needed is typically of the order* $1e^6$, *for obtaining an accuracy of* $1e^{-3}$ *in the solution vector.*

B.4 Proof-of-concept numerical simulations

In order to show the effectiveness of the proposed DyMonDS-based interactive scheme to solving an optimization problem coupled across multiple agents, we consider a communication network shown in Fig. 8.

It has two source-load pairs and the objective is to maximize the network utility. Each link has dedicated source power injections as shown in the Fig. 8 with an upper limit on

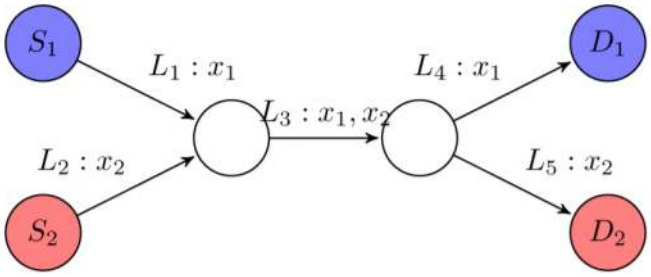

Fig. 8 Test network: Source destination pair is displayed with same color; $L_l : x_i, x_j \ldots$ denotes that the flow on link l is due to the flow from sources $i, j, \ldots$ [117]

the capacity of the flow through the wires. Let each of the sources have the utility functions $u_i(x_1) = C_i log(x_1 + 0.1)$ where $C_1 = 10$ and $C_2 = 20$. Let the set of sources be denoted using the set $\mathcal{S}$ and let the set of sources utilizing the link l be denoted using $\mathcal{S}(l)$. Similarly, let the length of the path in use by source i be denoted as $\mathcal{L}(i)$. Letting the capacity of all the links be equal to 1, the network utility maximization (NUM) problem can be posed as

$$\begin{aligned} &\max_{x} \sum_{i \in \mathcal{S}} C_i \log(x_1 + 0.1) \\ &\sum_{i \in \mathcal{S}(l)} x_i \leq 1 \qquad \forall l \in \mathcal{L} \\ &x_i \geq 0 \qquad \forall i \in \mathcal{S} \end{aligned} \tag{70}$$

In order to apply DyMonDS-based method, this formulation is a degenerate case of the one posed in Eqn. (36) where there are no internal constraints and all the variables appear the intersections. Thus, x_i in this formulation is to be treated like z_i in the formulation in Then the agent-specific formulation is to just optimize its own utility function given the lagrange multipliers corresponding to its coupling constraints. This can be posed as follows:

$$\begin{aligned} &\max_{x_i} C_i \log(x_i + 0.1) - \textstyle\sum_{j \in \mathcal{L}(i)} \lambda_j x_i \\ &x_i \geq 0 \end{aligned} \tag{71}$$

This problem is solved to obtain bids using the relations in Eqn. (50) which reduces to the following for this degenerate case of having no internal constraints

$$\frac{\partial B_i}{\partial x_i} = \underbrace{\nabla_x^2 f_i(y)}_{a_i^k} x_i + \underbrace{(\nabla_x f_i(y) - \nabla_x^2 f_i(y) y)}_{b_i^k} \tag{72}$$

Here $f_i(x_i) = C_i log(x_i + 0.1)$, y is the solution obtained by solving the agent level problem from λ^{k-1} in the previous iterate utilized to obtain the bid function for the next iteration. The bid constructed as $B_i^k(x_i) = \frac{1}{2} a_i^k x_i^2 + b_i^k x_i$, which are collected from all the sources and then optimized by the system coordinator by solving the following problem

$$\begin{aligned} &\max_{x} \sum_{i \in \mathcal{S}} B_i(x_i) \\ &\sum_{i \in \mathcal{S}(l)} x_i \leq 1 \qquad \forall l \in \mathcal{L} \\ &x_i \geq 0 \qquad \forall i \in \mathcal{S} \end{aligned} \tag{73}$$

Traditionally utilized first order gradient methods such as the distributed dual gradient and the fast dual gradient method are simulated for comparizon with the proposed DyMonDS-based approach. For the dual gradient algorithm and fast gradient algorithm, the step size for lagrange multiplier increments have been assumed to equal to $\alpha = \frac{2\sigma}{N_p} N_s$

where $\sigma = \nabla^2 f_i(1)$ is the strong convexity constant for the utility functions in used [117]. N_p and N_s respectively are the longest path lengths among all sources and maximum number of sources sharing particular link respectively.

For our DyMonDS approach, we do not have to go through the hassle of selecting a step-size however. For all the methods, all of the following termination conditions have been utilized [117]:

- primal objective function values satisfy $\left|\frac{f(x^{k+1})}{f(x^k)} - 1\right| \leq 0.01$
- dual variables satisfy the worst case differences $\|\lambda^{k+1} - \lambda^k\|_\infty \leq 0.01$
- primal feasibility satisfies $Ax^k - c < 0.01$ for all the links

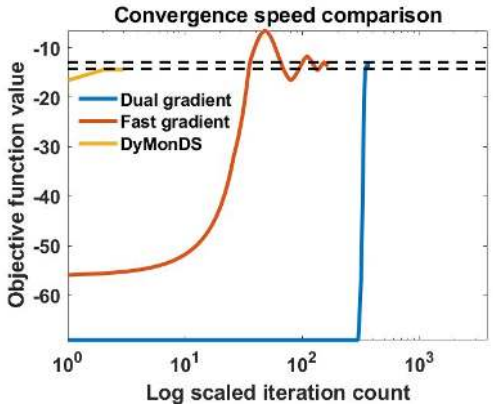

Fig. 9 Comparison of the rate of convergence of the proposed DyMonDS approach with that of two other distributed methods for a system with 2 sources and 5 links

All the tested methods converge to a value equal to $x_1 = 0.3$ and $x_2 = 0.7$ for when $C_1 = 10$ and $C_2 = 20$ in the utility functions used in the formulations of NUM in Eqn. (70). The convergence rates in terms of the objective function values for all three methods is shown in Fig. 9. Notice the effectiveness of the DyMonDS-based approach which only takes about 10 iterations for convergences in comparison to the other methods which can go upto thousands of iterations. Furthermore, just with a couple of iterations, the approach tends to converge to a near-optimal point which is permissible for large-scale systems.

Similar to the analysis in [117], we have further produced random networks with a random number of sources in the range $[1, 25]$ and a random number of links in the range of $[1, 40]$ in order to test the scalability. For each of the 50 trials performed, the number of iterations for convergence is shown in the Fig. 10. As anticipated the DyMonDS approach requires very few number of iterations irrespective of the size of the system.

References

1. Jin Wei and Deepa Kundur. Two-tier hierarchical cyber-physical security analysis framework for smart grid. In *2012 IEEE Power and Energy Society General Meeting*, pages 1–5. IEEE, 2012.
2. Marija D Ilić and Rupamathi Jaddivada. Multi-layered interactive energy space modeling for near-optimal electrification of terrestrial, shipboard and aircraft systems. *Annual Reviews in Control*, 45:52–75, 2018.
3. Marija D Ilic et al. Toward a unified modeling and control for sustainable and resilient electric energy systems. *Foundations and Trends® in Electric Energy Systems*, 1(1-2): 1–141, 2016.

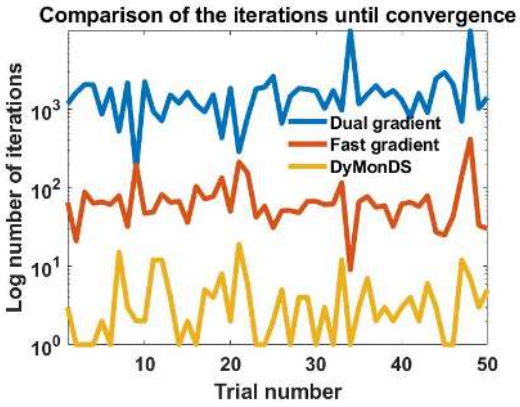

Fig. 10 Comparison of iterations for random network

4. Marija D Ilic and Rupamathi Jaddivada. Fundamental modeling and conditions for realizable and efficient energy systems. In *2018 IEEE Conference on Decision and Control (CDC)*, pages 5694–5701. IEEE, 2018.
5. Carnegie Mellon University Marija Ilic, Professor. Ferc reliability technical conference panel i: 2016 state of reliability.
6. Allen J Wood, Bruce F Wollenberg, and Gerald B Sheblé. *Power generation, operation, and control*. John Wiley & Sons, 2013.
7. Monica Chinchilla, Santiago Arnaltes, and Juan Carlos Burgos. Control of permanent-magnet generators applied to variable-speed wind-energy systems connected to the grid. *IEEE Transactions on energy conversion*, 21(1):130–135, 2006.
8. Biao Sun, Peter B Luh, Qing-Shan Jia, and Bing Yan. Event-based optimization within the lagrangian relaxation framework for energy savings in hvac systems. *IEEE Transactions on Automation Science and Engineering*, 12(4):1396–1406, 2015.
9. Bourhan Tashtoush, Mohammed Molhim, and Mohammed Al-Rousan. Dynamic model of an hvac system for control analysis. *Energy*, 30(10):1729–1745, 2005.
10. Ruisheng Diao, Shuai Lu, Marcelo Elizondo, Ebony Mayhorn, Yu Zhang, and Nader Samaan. Electric water heater modeling and control strategies for demand response. In *2012 IEEE power and energy society general meeting*, pages 1–8. IEEE, 2012.
11. Marija D Ilic and John Zaborszky. *Dynamics and control of large electric power systems*. Wiley New York, 2000.
12. Prabha Kundur, Neal J Balu, and Mark G Lauby. *Power system stability and control*, volume 7. McGraw-hill New York, 1994.
13. TA Rotting and A Gjelsvik. Stochastic dual dynamic programming for seasonal scheduling in the norwegian power system. *IEEE Transactions on Power Systems*, 7(1):273–279, 1992.
14. Federal Energy Regulatory Commission et al. Electric storage participation in markets operatied by regional transmission organization and independent system operators. *FERC. November*, 17, 2016.
15. Mehdi Dali, Jamel Belhadj, and Xavier Roboam. Hybrid solar–wind system with battery storage operating in grid-connected and standalone mode: control and energy management–experimental investigation. *Energy*, 35(6):2587–2595, 2010.
16. Olga Moraes Toledo, Delly Oliveira Filho, and Antônia Sônia Alves Cardoso Diniz. Distributed photovoltaic generation and energy storage systems: A review. *Renewable and Sustainable Energy Reviews*, 14(1):506–511, 2010.
17. Priyanka Paliwal, NP Patidar, and RK Nema. Planning of grid integrated distributed generators: A review of technology, objectives and techniques. *Renewable and sustainable energy reviews*, 40:557–570, 2014.

18. Bolun Xu, Magnus Korpas, Audun Botterud, and Francis O'Sullivan. A lagrangian policy for optimal energy storage control. *arXiv preprint arXiv:1901.09507*, 2019.
19. Jonathan Donadee and Marija D Ilić. Stochastic optimization of grid to vehicle frequency regulation capacity bids. *IEEE Transactions on Smart Grid*, 5(2), 2014.
20. Pierluigi Siano. Demand response and smart grids—a survey. *Renewable and sustainable energy reviews*, 30:461–478, 2014.
21. Qi Wang, Chunyu Zhang, Yi Ding, George Xydis, Jianhui Wang, and Jacob Østergaard. Review of real-time electricity markets for integrating distributed energy resources and demand response. *Applied Energy*, 138:695–706, 2015.
22. Daniele Zonetti, Romeo Ortega, and Johannes Schiffer. A tool for stability and power-sharing analysis of a generalized class of droop controllers for high-voltage direct-current transmission systems. *IEEE Transactions on Control of Network Systems*, 5 (3):1110–1119, 2017.
23. Sandeep Anand, Baylon G Fernandes, and Josep Guerrero. Distributed control to ensure proportional load sharing and improve voltage regulation in low-voltage dc microgrids. *IEEE Transactions on Power Electronics*, 28(4):1900–1913, 2012.
24. Claudio De Persis, Erik RA Weitenberg, and Florian Dörfler. A power consensus algorithm for dc microgrids. *Automatica*, 89:364–375, 2018.
25. Jianzhe Liu, Wei Zhang, and Giorgio Rizzoni. Robust stability analysis of dc microgrids with constant power loads. *IEEE Transactions on Power Systems*, 33(1):851–860, 2017.
26. Jorge Elizondo, Richard Y Zhang, Jacob K White, and James L Kirtley. Robust small signal stability for microgrids under uncertainty. In *2015 IEEE 6th International Symposium on Power Electronics for Distributed Generation Systems (PEDG)*, pages 1–8. IEEE, 2015.
27. Alan R Millner, Christopher L Smith, Rupamathi Jaddivada, and Marija D Ilić. Component standards for stable microgrids. *IEEE Transactions on Power Systems*, 34(2): 852–863, 2018.
28. Josep M Guerrero, Mukul Chandorkar, Tzung-Lin Lee, and Poh Chiang Loh. Advanced control architectures for intelligent microgrids—part i: Decentralized and hierarchical control. *IEEE Transactions on Industrial Electronics*, 60(4):1254–1262, 2012.
29. Reynaldo Salcedo, Edward Corbett, Christopher Smith, Erik Limpaecher, Raajiv Rekha, John Nowocin, Georg Lauss, Edwin Fonkwe, Murilo Almeida, Peter Gartner, et al. Banshee distribution network benchmark and prototyping platform for hardware-in-the-loop integration of microgrid and device controllers. *The Journal of Engineering*, 2019.
30. Mads Almassalkhi, Jeff Frolik, and Paul Hines. Packetized energy management: asynchronous and anonymous coordination of thermostatically controlled loads. In *2017 American Control Conference (ACC)*, pages 1431–1437. IEEE, 2017.
31. Wei Zhang, Karanjit Kalsi, Jason Fuller, Marcelo Elizondo, and David Chassin. Aggregate model for heterogeneous thermostatically controlled loads with demand response. In *2012 IEEE Power and Energy Society General Meeting*, pages 1–8. IEEE, 2012.
32. Thomas Navidi, Abbas El Gamal, and Ram Rajagopal. A two-layer decentralized control architecture for der coordination. In *2018 IEEE Conference on Decision and Control (CDC)*, pages 6019–6024. IEEE, 2018.
33. Grayson C Heffner, Charles A Goldman, and Mithra M Moezzi. Innovative approaches to verifying demand response of water heater load control. *IEEE Transactions on Power Delivery*, 21(1):388–397, 2005.
34. Joy Chandra Mukherjee and Arobinda Gupta. A review of charge scheduling of electric vehicles in smart grid. *IEEE Systems Journal*, 9(4):1541–1553, 2014.
35. Daniel K Molzahn, Ian A Hiskens, et al. A survey of relaxations and approximations of the power flow equations. *Foundations and Trends® in Electric Energy Systems*, 4(1-2):1–221, 2019.
36. Xuan Zhang, Wenbo Shi, Bin Yan, Ali Malkawi, and Na Li. Decentralized and distributed temperature control via hvac systems in energy efficient buildings. *arXiv preprint arXiv:1702.03308*, 2017.
37. Changhong Zhao, Emiliano Dall'Anese, and Steven H Low. Convex relaxation of opf in multiphase radial networks with delta connection. In *Proceedings of the 10th Bulk*

Power Systems Dynamics and Control Symposium, 2017.
38. Carleton Coffrin and Pascal Van Hentenryck. A linear-programming approximation of ac power flows. *INFORMS Journal on Computing*, 26(4):718–734, 2014.
39. Marija IliC. Network theoretic conditions for existence and uniqueness of steady state solutions to electric power circuits. In *[Proceedings] 1992 IEEE International Symposium on Circuits and Systems*, volume 6, pages 2821–2828. IEEE, 1992.
40. Florian Dörfler and Francesco Bullo. Novel insights into lossless ac and dc power flow. In *2013 IEEE Power & Energy Society General Meeting*, pages 1–5. IEEE, 2013.
41. Renato BL Guedes, Luis FC Alberto, and Newton G Bretas. Power system low-voltage solutions using an auxiliary gradient system for voltage collapse purposes. *IEEE Transactions on Power Systems*, 20(3):1528–1537, 2005.
42. Yang Feng. *Solving for the Low-Voltage/Large-Angle Power-Flow Solutions by Using the*. PhD thesis, Arizona State University, 2015.
43. Weimin Ma and James S Thorp. An efficient algorithm to locate all the load flow solutions. *IEEE Transactions on Power Systems*, 8(3):1077–1083, 1993.
44. Dhagash Mehta, Daniel K Molzahn, and Konstantin Turitsyn. Recent advances in computational methods for the power flow equations. In *2016 American Control Conference (ACC)*, pages 1753–1765. IEEE, 2016.
45. Matt Kraning, Eric Chu, Javad Lavaei, Stephen Boyd, et al. Dynamic network energy management via proximal message passing. *Foundations and Trends® in Optimization*, 1(2):73–126, 2014.
46. Na Li, Guannan Qu, and Munther Dahleh. Real-time decentralized voltage control in distribution networks. In *2014 52nd Annual Allerton Conference on Communication, Control, and Computing (Allerton)*, pages 582–588. IEEE, 2014.
47. Qiuyu Peng and Steven H Low. Distributed optimal power flow algorithm for radial networks, i: Balanced single phase case. *IEEE Transactions on Smart Grid*, 9(1): 111–121, 2016.
48. Xinyang Zhou, Emiliano Dall'Anese, Lijun Chen, and Andrea Simonetto. An incentive-based online optimization framework for distribution grids. *IEEE transactions on Automatic Control*, 63(7):2019–2031, 2017.
49. Haoyu Yuan, Fangxing Li, Yanli Wei, and Jinxiang Zhu. Novel linearized power flow and linearized opf models for active distribution networks with application in distribution lmp. *IEEE Transactions on Smart Grid*, 9(1):438–448, 2016.
50. Dimitris Bertsimas, Eugene Litvinov, Xu Andy Sun, Jinye Zhao, and Tongxin Zheng. Adaptive robust optimization for the security constrained unit commitment problem. *IEEE transactions on power systems*, 28(1):52–63, 2012.
51. Jean Pauphilet, Diego Kiner, Damien Faille, and Laurent El Ghaoui. A tractable numerical strategy for robust milp and application to energy management. In *2016 IEEE 55th Conference on Decision and Control (CDC)*, pages 1490–1495. IEEE, 2016.
52. Burak Kocuk, Santanu S Dey, and X Andy Sun. Strong socp relaxations for the optimal power flow problem. *Operations Research*, 64(6):1177–1196, 2016.
53. Zhiwei Xu, Duncan S Callaway, Zechun Hu, and Yonghua Song. Hierarchical coordination of heterogeneous flexible loads. *IEEE Transactions on Power Systems*, 31(6): 4206–4216, 2016.
54. Balho H Kim and Ross Baldick. A comparison of distributed optimal power flow algorithms. *IEEE Transactions on Power Systems*, 15(2):599–604, 2000.
55. Magnus R Hestenes. Multiplier and gradient methods. *Journal of optimization theory and applications*, 4(5):303–320, 1969.
56. Ermin Wei and Asuman Ozdaglar. Distributed alternating direction method of multipliers. In *2012 IEEE 51st IEEE Conference on Decision and Control (CDC)*, pages 5445–5450. IEEE, 2012.
57. Albert Lam, Alejandro Dominguez-Garcia, Baosen Zhang, and David Tse. Optimal distributed voltage regulation in power distribution networks. Technical report, 2012.
58. Albert YS Lam, Baosen Zhang, and N Tse David. Distributed algorithms for optimal power flow problem. In *2012 IEEE 51st IEEE Conference on Decision and Control (CDC)*, pages 430–437. IEEE, 2012.
59. Gabriela Hug-Glanzmann and Göran Andersson. Decentralized optimal power flow control for overlapping areas in power systems. *IEEE Transactions on Power Systems*,

24(1):327–336, 2009.
60. Emiliano Dall'Anese, Hao Zhu, and Georgios B Giannakis. Distributed optimal power flow for smart microgrids. *IEEE Transactions on Smart Grid*, 4(3):1464–1475, 2013.
61. Daniel K Molzahn, Florian Dörfler, Henrik Sandberg, Steven H Low, Sambuddha Chakrabarti, Ross Baldick, and Javad Lavaei. A survey of distributed optimization and control algorithms for electric power systems. *IEEE Transactions on Smart Grid*, 8(6):2941–2962, 2017.
62. Yamin Wang, Lei Wu, and Shouxiang Wang. A fully-decentralized consensus-based admm approach for dc-opf with demand response. *IEEE Transactions on Smart Grid*, 8(6):2637–2647, 2016.
63. Angel Molina-Garcia, François Bouffard, and Daniel S Kirschen. Decentralized demand-side contribution to primary frequency control. *IEEE Transactions on Power Systems*, 26(1):411–419, 2010.
64. Ruiwei Jiang, Jianhui Wang, and Yongpei Guan. Robust unit commitment with wind power and pumped storage hydro. *IEEE Transactions on Power Systems*, 27(2):800–810, 2011.
65. Michal Melamed, Aharon Ben-Tal, and Boaz Golany. A multi-period unit commitment problem under a new hybrid uncertainty set for a renewable energy source. *Renewable energy*, 118:909–917, 2018.
66. Long Zhao and Bo Zeng. Robust unit commitment problem with demand response and wind energy. In *2012 IEEE power and energy society general meeting*, pages 1–8. IEEE, 2012.
67. Le Xie, Yingzhong Gu, Xinxin Zhu, and Marc G Genton. Short-term spatio-temporal wind power forecast in robust look-ahead power system dispatch. *IEEE Transactions on Smart Grid*, 5(1):511–520, 2013.
68. Chaoyue Zhao, Jianhui Wang, Jean-Paul Watson, and Yongpei Guan. Multi-stage robust unit commitment considering wind and demand response uncertainties. *IEEE Transactions on Power Systems*, 28(3):2708–2717, 2013.
69. Luis A Duffaut Espinosa, Mads Almassalkhi, Paul Hines, Shoeib Heydari, and Jeff Frolik. Towards a macromodel for packetized energy management of resistive water heaters. In *2017 51st Annual Conference on Information Sciences and Systems (CISS)*, pages 1–6. IEEE, 2017.
70. Wei Zhang, Karanjit Kalsi, Jason Fuller, Marcelo Elizondo, and David Chassin. Aggregate model for heterogeneous thermostatically controlled loads with demand response. In *2012 IEEE Power and Energy Society General Meeting*, pages 1–8. IEEE, 2012.
71. Borhan M Sanandaji, He Hao, and Kameshwar Poolla. Fast regulation service provision via aggregation of thermostatically controlled loads. In *2014 47th Hawaii International Conference on System Sciences*, pages 2388–2397. IEEE, 2014.
72. Anupam A Thatte, Le Xie, Daniel E Viassolo, and Sunita Singh. Risk measure based robust bidding strategy for arbitrage using a wind farm and energy storage. *IEEE Transactions on Smart Grid*, 4(4):2191–2199, 2013.
73. Noemi G Cobos, José M Arroyo, Natalia Alguacil, and Jianhui Wang. Robust energy and reserve scheduling considering bulk energy storage units and wind uncertainty. *IEEE Transactions on Power Systems*, 33(5):5206–5216, 2018.
74. Zhi Chen, Lei Wu, and Yong Fu. Real-time price-based demand response management for residential appliances via stochastic optimization and robust optimization. *IEEE Transactions on Smart Grid*, 3(4):1822–1831, 2012.
75. Tianyi Chen, Na Li, and Georgios B Giannakis. Aggregating flexibility of heterogeneous energy resources in distribution networks. In *2018 Annual American Control Conference (ACC)*, pages 4604–4609. IEEE, 2018.
76. Ponpranod Didsayabutra, Wei-Jen Lee, and Bundhit Eua-Arporn. Defining the must-run and must-take units in a deregulated market. *IEEE transactions on industry applications*, 38(2):596–601, 2002.
77. Paul R Gribik, William W Hogan, and Susan L Pope. Market-clearing electricity prices and energy uplift. *Cambridge, MA*, 2007.
78. José Manuel Arroyo and Antonio J Conejo. Multiperiod auction for a pool-based electricity market. *IEEE Transactions on Power Systems*, 17(4):1225–1231, 2002.

79. Peter B Luh, William E Blankson, Ying Chen, Joseph H Yan, Gary A Stern, Shi-Chung Chang, and Feng Zhao. Payment cost minimization auction for deregulated electricity markets using surrogate optimization. *IEEE Transactions on Power systems*, 21(2): 568–578, 2006.
80. Alexander Martin, Johannes C Müller, and Sebastian Pokutta. Strict linear prices in non-convex european day-ahead electricity markets. *Optimization Methods and Software*, 29(1):189–221, 2014.
81. Carlos Ruiz, Antonio J Conejo, and Steven A Gabriel. Pricing non-convexities in an electricity pool. *IEEE Transactions on Power Systems*, 27(3):1334–1342, 2012.
82. Arjen A van der Meer, Madeleine Gibescu, Mart AMM van der Meijden, Wil L Kling, and Jan A Ferreira. Advanced hybrid transient stability and emt simulation for vsc-hvdc systems. *IEEE Transactions on Power Delivery*, 30(3):1057–1066, 2014.
83. LL Grant, ML Crow, and Maggie Xiaoyan Cheng. Computationally efficient solvers for power system applications. In *2015 IEEE Power and Energy Conference at Illinois (PECI)*, pages 1–5. IEEE, 2015.
84. Miloč Cvetković and Marija Ilić. Interaction variables for distributed numerical integration of nonlinear power system dynamics. In *2015 53rd Annual Allerton Conference on Communication, Control, and Computing (Allerton)*, pages 560–566. IEEE, 2015.
85. MD Omar Faruque, Thomas Strasser, Georg Lauss, Vahid Jalili-Marandi, Paul Forsyth, Christian Dufour, Venkata Dinavahi, Antonello Monti, Panos Kotsampopoulos, Juan A Martinez, et al. Real-time simulation technologies for power systems design, testing, and analysis. *IEEE Power and Energy Technology Systems Journal*, 2(2):63–73, 2015.
86. Christian Dufour, Simon Abourida, and Jean Belanger. Hardware-in-the-loop simulation of power drives with rt-lab. In *2005 International Conference on Power Electronics and Drives Systems*, volume 2, pages 1646–1651. IEEE, 2005.
87. Sang-Jin Oh, Cheol-Hee Yoo, Il-Yop Chung, and Dong-Jun Won. Hardware-in-the-loop simulation of distributed intelligent energy management system for microgrids. *Energies*, 6(7):3263–3283, 2013.
88. RO Salcedo, JK Nowocin, CL Smith, RP Rekha, EG Corbett, ER Limpaecher, and JM LaPenta. Development of a real-time hardware-in-the-loop power systems simulation platform to evaluate commercial microgrid controllers. Technical report, Massachusetts Inst of Tech Lexington Lincoln lab, 2016.
89. Ruben Pena, JC Clare, and GM Asher. Doubly fed induction generator using back-to-back pwm converters and its application to variable-speed wind-energy generation. *IEE Proceedings-Electric Power Applications*, 143(3):231–241, 1996.
90. Marija Ilić, Rupamathi Jaddivada, and Xia Miao. Modeling and analysis methods for assessing stability of microgrids. *IFAC-PapersOnLine*, 50(1):5448–5455, 2017.
91. Kevin D Bachovchin and Marija D Ilić. Automated modeling of power system dynamics using the lagrangian formulation. *International Transactions on Electrical Energy Systems*, 25(10):2087–2108, 2015.
92. Abraham Jan van der Schaft and AJ Van Der Schaft. *L2-gain and passivity techniques in nonlinear control*, volume 2. Springer, 2000.
93. JL Wyatt and M Ilic. Time-domain reactive power concepts for nonlinear, nonsinusoidal or nonperiodic networks. In *IEEE International Symposium on Circuits and Systems*, pages 387–390. IEEE, 1990.
94. Krishna Chaitanya Kosaraju, Ramkrishna Pasumarthy, Navdeep M Singh, and Alexander L Fradkov. Control using new passivity property with differentiation at both ports. In *2017 Indian Control Conference (ICC)*, pages 7–11. IEEE, 2017.
95. Charles A Desoer and Jacob Katzenelson. Nonlinear rlc networks. *Bell System Technical Journal*, 44(1):161–198, 1965.
96. Marija D Ilić and Qixing Liu. Toward sensing, communications and control architectures for frequency regulation in systems with highly variable resources. In *Control and Optimization Methods for Electric Smart Grids*, pages 3–33. Springer, 2012.
97. Marija D Ilic. From hierarchical to open access electric power systems. *Proceedings of the IEEE*, 95(5):1060–1084, 2007.
98. Xia Miao, Qixing Liu, and Marija Ilic. Enhanced automatic generation control (e-agc) for electric power systems with large intermittent renewable energy sources. *arXiv preprint arXiv:1902.07644*, 2019.

99. Paul Penfield, Robert Spence, and Simon Duinker. A generalized form of tellegen's theorem. *IEEE Transactions on Circuit Theory*, 17(3):302–305, 1970.
100. Changhong Zhao, Ufuk Topcu, Na Li, and Steven Low. Design and stability of load-side primary frequency control in power systems. *IEEE Transactions on Automatic Control*, 59(5):1177–1189, 2014.
101. Paul Denholm, Matthew O'Connell, Gregory Brinkman, and Jennie Jorgenson. Overgeneration from solar energy in california. a field guide to the duck chart. Technical report, National Renewable Energy Lab.(NREL), Golden, CO (United States), 2015.
102. Nipun Popli and Marija D Ilić. Enabling convex energy bids for flexible ramp product via smart local automation. *IFAC-PapersOnLine*, 48(30):245–250, 2015.
103. Joe H Chow, G Peponides, PV Kokotovic, B Avramovic, and JR Winkelman. *Time-scale modeling of dynamic networks with applications to power systems*, volume 46. Springer, 1982.
104. Marija lic and Rupamathi Jaddivada. Toward technically feasible and economically efficient integration of distributed energy resources. In *57th Annual Allerton Conference on Communication, Control, and Computing 2019*. University of Illinois at Urbana-Champaign, Coordinated Science Laboratory . . . (To Appear), 2019.
105. Xia Miao and Marija D Ilić. Model predictive excitation control for constrained frequency and voltage stabilization. In *2015 IEEE Power & Energy Society General Meeting*, pages 1–5. IEEE, 2015.
106. Xia Miao and Marija D Ilić. Distributed model predictive control of synchronous machines for stabilizing microgrids. In *2017 North American Power Symposium (NAPS)*, pages 1–6. IEEE, 2017.
107. Marija Ilic, MIAO Xia, and Rupamathi Jaddivada. Plug-and-play reconfigurable electric power microgrids, November 1 2018. US Patent App. 15/965,823.
108. JW Chapman, MD Ilic, CA King, L Eng, and H Kaufman. Stabilizing a multimachine power system via decentralized feedback linearizing excitation control. *IEEE Transactions on Power Systems*, 8(3):830–839, 1993.
109. Niels LaWhite and Marija D Ilic. Vector space decomposition of reactive power for periodic nonsinusoidal signals. *IEEE Transactions on Circuits and Systems I: Fundamental Theory and Applications*, 44(4):338–346, 1997.
110. Marija D Ilic and Rupamathi Jaddivada. Exergy/energy dynamics-based integrative modeling and control method for difficult electric aircraft missions, September 12 2019. Provisional Patent Application No. 62/730203.
111. Marija Dragoljub Ilic, Jhi Young Joo, Burton Warren Andrews, Badri Raghunathan, Diego Benitez, and Felix Maus. Adaptive load management: a system for incorporating customer electrical demand information for demand and supply side energy management, April 5 2012. US Patent App. 12/895,780.
112. Victor M Zavala. New architectures for hierarchical predictive control. *IFAC-PapersOnLine*, 49(7):43–48, 2016.
113. Marija Ilic, Rupamathi Jaddivada, Xia Miao, and Nipun Popli. Toward multi-layered mpc for complex electric energy systems. In *Handbook of Model Predictive Control*, pages 625–663. Springer, 2019.
114. Nipun Popli, Rupamathi Jaddivada, Francis O'Sullivan, and Marija Ilic. Accommodating wind and solar in low-flexibility systems: Unbundling flexibilities for sequential dispatch. *IEEE Transactions on Power Systems*, 2019 (Submitted).
115. Paul J Werbos. Ai intelligence for the grid 16 years later: progress, challenges and lessons for other sectors. In *2018 International Joint Conference on Neural Networks (IJCNN)*, pages 1–8. IEEE, 2018.
116. Amir Beck and Marc Teboulle. A fast iterative shrinkage-thresholding algorithm for linear inverse problems. *SIAM journal on imaging sciences*, 2(1):183–202, 2009.
117. Amir Beck, Angelia Nedić, Asuman Ozdaglar, and Marc Teboulle. An $o(1/k)$ gradient method for network resource allocation problems. *IEEE Transactions on Control of Network Systems*, 1(1):64–73, 2014.